Hans-Georg Weber
Masataka Nakazawa

OPTICAL AND FIBER COMMUNICATIONS REPORTS 3

Ultrahigh-Speed Optical Transmission Technology

Springer

Hans-Georg Weber Masataka Nakazawa
Editors

Ultrahigh-Speed Optical Transmission Technology

With 350 Figures

Springer

Hans-Georg Weber
Fraunhofer Institute for
Telecommunications
Heinrich-Hertz-Institut
Einsteinufer 37
10587 Berlin, Germany
hgweber@hhi.fhg.de

Masataka Nakazawa
Research Institute of Electrical
Communication
2-1-1 Katahira
Sendai-shi, Miyagiken 980-8577
Aoba-Ka, Japan
nakazawa@riec.tohoku.ac.jp

Library of Congress Control Number:

ISBN-13: 978-3-540-23878-2 e-ISBN-13: 978-3-540-68005

Printed on acid-free paper.

9 8 7 6 5 4 3 2 1

springer.com

Contents

Introduction to ultra-high-speed optical transmission technology

Hans-Georg Weber[1] and Masataka Nakazawa[2]

[1] Fraunhofer Institute for Telecommunications, Heinrich-Hertz-Institut
Einsteinufer 37, 10587 Berlin, Germany
Email: hgweber@hhi.fhg.de
[2] Research Institute of Electrical Communication, Tohoku University
2-1-1 Katahira, Aoba-ku, Sendai-shi, Miyagi-ken 980-8577, Japan
Email: nakazawa@riec.tohoku.ac.jp

Abstract. This paper serves as an introduction to this volume on ultra-high-speed optical transmission technology. It reviews ultra-high-speed data transmission in optical fibers, which is essentially the same as optical time division multiplexing (OTDM) transmission technology. The research work in this field is driven by the need to increase the transmission capacity and controllability of fiber optic networks as well as by an interest in investigating the feasibility of high-speed data transmission in fiber. The chapter summarizes OTDM components and describes results of OTDM-transmission experiments. In addition, it outlines the chapters of this volume, which describe the considered topics in detail.

1. The Challenge of OTDM

The rapid increase in data traffic in communication networks has led to a demand for higher transmission capacities. New fibers may need to be installed from time to time. However, the costs are high and lead times may be long. Therefore, finding a way to increase the fiber transmission capacity is the target of many studies. The transmission capacity per fiber is given by the number of wavelength division multiplexing (WDM) channels multiplied by the time division multiplexing (TDM) bit rate per channel. The past has seen considerable interest in the use of WDM to increase the total transmission capacity. For instance, a 10-Tbit/s transmission capacity was achieved in 2001 using WDM systems with about 260 wavelength channels and a TDM bit rate of 40 Gbit/s [1,2]. However, for very large numbers of wavelength channels (e.g., a few thousand), such factors as wavelength management, power consumption, and footprint will probably limit the usefulness of increasing the number of WDM channels

and will favor a higher TDM bit rate in terms of increasing the total transmission capacity. The motivation for higher TDM bit rates also arises from the effort to reduce the cost per transmitted information bit. A higher TDM bit rate will make it possible to reduce the number of transmitters and receivers and to increase both the spectral and space efficiency of WDM systems. Indeed, in the past the TDM bit rate was steadily increased in installed fiber transmission systems. In the early 1990s and in about 1995, respectively, TDM bit rates of 2.5 and 10 Gbit/s were introduced in commercial fiber transmission systems. This TDM bit rate has now been increased to 40 Gbit/s. These bit rates are all based on electrical signal processing (electrical TDM, ETDM). The next generation TDM bit rate will be 160 Gbit/s. As electrical signal processing is currently unavailable at this bit rate, many laboratories are investigating optical TDM (OTDM) technology. The basics of OTDM technology have been described in several review articles [3–5] and will be discussed below.

The most challenging view as regards OTDM technology is that optical networks will evolve into "photonic networks", in which ultrafast optical signals of any bit rate and modulation format will be transmitted and processed from end to end without optical-electrical-optical conversion. With this as the target, OTDM technology presents us with the challenge of investigating and developing high-speed optical signal processing and exploring the ultimate capacity for fiber transmission in a single wavelength channel. We must study how the advantages of high TDM bit rates are eventually eroded by an increase in detrimental effects. A higher TDM bit rate makes transmission systems more vulnerable to chromatic dispersion (CD) and polarization-mode dispersion (PMD), as well as creating the need for a higher optical signal-to-noise ratio (OSNR) in the wavelength channel. A higher OSNR is obtained by employing a higher signal power, and this will make the system more sensitive to fiber non-linearity. On the other hand, the need for a high signal power may be reduced by other means such as distributed Raman amplification, advanced optical modulation formats and the use of forward error correction (FEC).

From another viewpoint, OTDM technology is considered to be an interim technique with which to study high-speed data transmission in fiber. In this sense, OTDM will be replaced by ETDM as soon as electrical signal processing becomes available at the required TDM bit rate. This is currently the case with a TDM bit rate of 40 Gbit/s and will probably reach a TDM bit rate of 160 Gbit/s in the future. Recent advances in high-speed electronic ICs based on SiGe technology [6], broadband low drive voltage modulators [7] and waveguide pin detectors [8] indicate that full electronic TDM systems operating at 80 Gbit/s and above are already feasible. For example, an ETDM receiver working at 85 Gbit/s has recently been demonstrated [9]. From this standpoint, the main task as regards OTDM technology is to investigate the feasibility of ultrahigh-speed data transmission as a prerequisite to the development of ETDM technology.

The "photonic network" appears to be a task for the distant future and ETDM technology will dominate commercial transmission systems in the near future. Nevertheless, some OTDM components may find applications in current ETDM systems. Optical pulse sources will be used in ETDM systems with an RZ-modulation format. OTDM demultiplexers already perform better than ETDM receivers at data rates of 80 Gbit/s. We may expect communication networks to be based on an appropriate combination of WDM, ETDM and OTDM technologies. Also, OTDM components, such

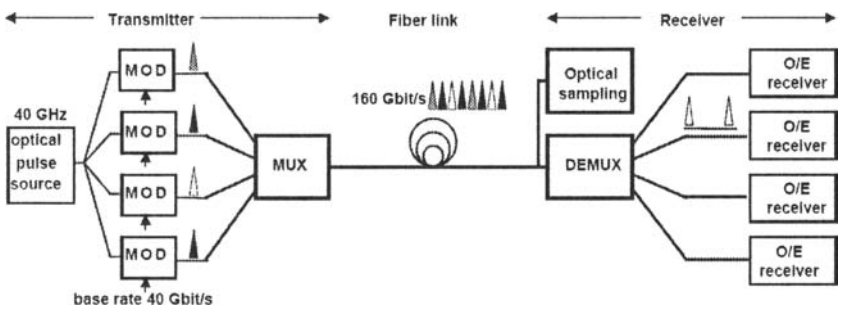

Fig. 1. Schematic view of a 160-Gbit/s OTDM transmission system.

as pulse sources, optical gates and clock recovery devices are already being employed in optical sampling systems for waveform and signal quality monitoring.

2. OTDM Transmission System

Figure 1 is a schematic illustration of a 160-Gbit/s OTDM transmission system as an example. The essential component on the transmitter side is an optical pulse source. The repetition frequency of a generated pulse train depends on the base data rate (ETDM data rate). The system shown in Fig. 1 has a base data rate of 40 Gbit/s. The 40-GHz optical pulse train is coupled into four optical branches, in which modulators (MOD) driven by 40 Gbit/s electrical data signals generate 40 Gbit/s optical return to zero (RZ) data signals. The modulation formats include on-off keying (OOK), differential phase shift keying (DPSK), and differential quadrature phase shift keying (DQPSK). The format depends on the modulation format of the electrical data signal and the appropriate modulator. The four optical data signals (TDM channels) are bit-interleaved by a multiplexer (MUX) to generate a multiplexed 160-Gbit/s optical data signal. Multiplexing can be such that all bits of the multiplexed data signal have the same polarization (SP multiplexing) or adjacent bits have alternating (orthogonal) polarization (AP multiplexing). Moreover, the controllability of the optical phases of pulses in adjacent bit slots is an important feature of an OTDM system. On the receiver side, the essential component is an optical demultiplexer (DEMUX), which separates the four base rate data signals (TDM channels) for subsequent detection and electrical signal processing.

The laboratory systems described in this book are frequently simplified on the transmitter side by adopting a set-up with only one modulator, which is combined with a pulse source for a 40-Gbit/s optical transmitter. This optical data signal is then multiplexed by a fiber delay line multiplexer to a 160-Gbit/s data signal using SP or AP multiplexing (see Fig. 2). The laboratory systems described in this book are also frequently simplified on the receiver side. That is, only one 40-Gbit/s TDM channel is selected and detected by one 40-Gbit/s optoelectric receiver at a given time. In a proper experiment all TDM channels are measured successively in this way.

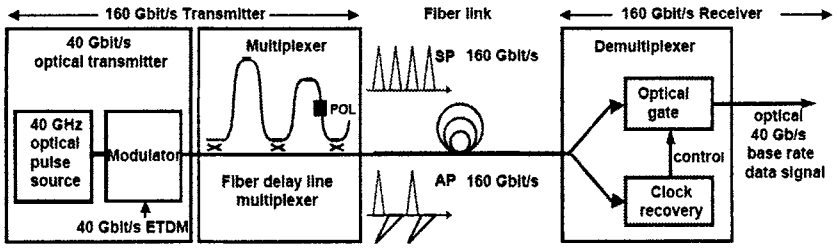

Fig. 2. Schematic view of a simplified 160-Gbit/s OTDM transmission system.

The DEMUX shown in Fig. 2 comprises two parts, an optical gate and a clock recovery device. The optical gate is a fast switch with a switching time that is shorter than the bit period (6.25 ps for 160 Gbit/s) of the multiplexed data signal. The clock recovery device provides the timing signal for the optical gate. Very often in papers on OTDM technology, the DEMUX is identified with the optical gate, and the clock recovery is considered as a separate unit next to the DEMUX.

The transmission system must be capable of compensating for chromatic dispersion (CD) and polarization mode dispersion (PMD), which both depend on the type of single-mode fiber used in the transmission system. For advanced high-speed transmission systems, it is desirable to employ techniques such as optical sampling to monitor the optical data signal with picosecond resolution. Chapter 17 ("Optical sampling techniques", by Schmidt-Langhorst and Weber) reviews the techniques used in optical sampling systems to perform the ultrafast sampling of the signal under investigation.

For even more advanced systems, high-speed optical signal processing techniques must be developed not only for the point-to-point transmission shown in Fig. 1, but also for transmission nodes. Components and subsystems such as add-drop multiplexers [e.g., 10–13], wavelength converters [e.g., 14–17], modulation format converters [e.g., 18] and optical regenerators [e.g., 19,20] are also required. These topics are partly dealt with in chapter 6 ("Optical signal processing using nonlinear fibers", by Watanabe) in the context of fiber-based optical signal processing and in chapters 5 ("High-speed optical signal processing using semiconductor optical amplifiers", by Schubert et al.) and 8 ("Optical nonlinearities in semiconductor optical amplifier and electro-absorption modulator: their applications to all-optical regeneration", by Usami and Nishimura) in the context of semiconductor optical amplifier and electroabsorption modulator based optical signal processing.

Figures 1 and 2 show the set-up of a one wavelength channel OTDM system. Chapters 13 ("Application of electroabsorption modulators for high-speed transmission systems", by Lach et al.) and 15 ("Ultrafast optical technologies for large-capacity TDM/WDM photonic networks", by Morioka) also provide examples of WDM/OTDM transmission systems comprising several wavelength channels.

3. Transmitter: Optical Pulse Source, Modulator, Multiplexer

High bit rate transmission demands reliable short pulse generation at high repetition frequencies. The pulse source must provide the following: a well-controlled repetition frequency and wavelength, transform limited pulses, a pulse width shorter than the bit period of the multiplexed data signal, a timing jitter much less than the pulse width, low amplitude noise, and a high extinction ratio (pedestal suppression). The pulse width should be less than one quarter of the bit period (1.5 ps for 160 Gbit/s) for SP multiplexing and less than one half of the bit period for AP multiplexing to avoid coherent beat noise between adjacent bits. Moreover, if some sort of phase modulation format such as a DPSK is used, there are further pulse source requirements, namely it must be highly stable in terms of phase and carrier wavelength.

Various pulse sources were used in the OTDM transmission experiments. Semiconductor mode-locked lasers (ML-LD) are becoming increasingly attractive, as they are stable, compact and viable for OTDM applications. In chapter 2 ("Semiconductor mode-locked lasers as pulse sources for high bit rate data transmission", by Jiang et al.), the ML-LD is evaluated as a pulse source for high bit rate data transmission. This chapter compares various OTDM source technologies, explains the impact of timing jitter and amplitude noise on OTDM performance, and illustrates how to characterize OTDM source noise. Another important pulse source is the mode-locked fiber ring laser (ML-FRL). Chapter 3 ("Ultrafast mode-locked fiber lasers for high-speed OTDM transmission and related topics", by Nakazawa) provides a detailed description of several types of ML-FRL, which are capable of generating picosecond to femtosecond optical pulse trains at repetition rates of 10 to 40 GHz in the 1.55 μm region. The ML-FRL is a harmonically mode-locked laser, whereas the ML-LD is generally operated at the fundamental mode repetition frequency. Recently, a solid-state mode-locked laser, known as an erbium-glass oscillator pulse generating laser (ERGO-PGL), was successfully operated in a 160 Gbit/s transmission experiment [12]. This laser operates at the fundamental mode repetition frequency. It has very low amplitude and phase noise and a pulse width that is slightly larger than those of the ML-LD and ML-FRL.

Another pulse source is a CW laser externally modulated (CW-Mod) by a Mach-Zehnder modulator or an electroabsorption modulator (EAM). The application of this pulse source in 160 and 320 Gbit/s (AP multiplexing) OTDM transmission experiments is described in chapter 13 ("Application of electroabsorption modulators for high-speed transmission systems", by Lach et al.). In general this type of pulse source does not provide optical pulses with a pulse width of less than about 3 ps. Some sort of subsequent pulse compression (PuC) and optical regeneration are needed to generate shorter pulses.

A pulse source of particular interest for WDM/OTDM applications is the supercontinuum pulse generation (SC-pulse) described in chapter 15 ("Ultrafast optical technologies for large-capacity TDM/WDM photonic networks", by Morioka). This pulse source provides short (<1 ps) optical pulses, whose pulse width and wavelength are both tunable. Moreover, this pulse source can be used as a multi-wavelength pulse source for WDM/OTDM systems.

The generated pulse train is modulated by using an EAM or a lithium-niobate ($LiNbO_3$) modulator. Chapter 4 ("Ultra-high-speed $LiNbO_3$ modulators", by Noguchi) discusses state of the art ultrahigh-speed $LiNbO_3$ modulators. The $LiNbO_3$ modulator covers a very broad band. Moreover, its modulation characteristics, such as insertion

loss, driving voltage (half-wave voltage), and frequency response, have little dependence on wavelength in the 1.3 to 1.5 μm range. In addition, the frequency chirping of a modulated optical signal can be reduced to almost zero. $LiNbO_3$ modulators have been used as amplitude and phase modulators in many high bit rate transmission experiments. Chapter 13 ("Application of electroabsorption modulators for high-speed transmission systems", by Lach et al.) describes the application of the EAM in OTDM experiments for data modulation as well as pulse carving, and this chapter also compares the EAM and the $LiNbO_3$ modulator.

Most optical multiplexers (MUX) are of the kind depicted in Fig. 2. They are realized by using 2×2 optical couplers and optical delay lines either as fiber devices or as planar lightwave circuits. These multiplexers are not "real" multiplexers, which combine TDM channels generated, for example, by different modulators (see Fig. 1) to provide a multiplexed data signal. The delay line multiplexers generate a high bit rate test signal for laboratory experiments by combining several replicas of one data signals with different relative delays. An important requirement for these "test multiplexers" is that there is no correlation between the adjacent bits of the multiplexed data signal. This is obtained by employing a delay time, which is long compared with the bit period of the input signal. These test multiplexers are described in more detail in chapter 13 ("Application of electroabsorption modulators for high-speed transmission systems", by Lach et al.). An example of a "real" multiplexer is provided in chapter 15 ("Ultrafast optical technologies for large-capacity TDM/WDM photonic networks", by Morioka). This multiplexer enables the multiplexing of eight different 20 Gbit/s data signals to one multiplexed 160 Gbit/s data signal by using an integrated planar lightwave circuit [21, 22]. Yet another "real" multiplexer is reported in [23] and described in chapter 13 ("Application of electroabsorption modulators for high-speed transmission systems", by Lach et al.). It provides independent modulation of all TDM-channels and optical phase alignment between adjacent bits.

4. OTDM-Receiver: Optical Demultiplexer, Clock Recovery Device, O/E-Receiver

Various switching devices have been used for demultiplexing. In very high-speed transmission experiments, optical switching was based on fiber nonlinearity using cross phase modulation (XPM) or four wave mixing (FWM) in fibers [3–5]. A well-known example is the nonlinear optical loop mirror (NOLM) [24]. Chapter 14 ("Ultrafast OTDM transmission using novel fiber devices for pulse compression, shaping, and demultiplexing", by Yamamoto and Nakazawa) describes the application of the NOLM as a DEMUX for a data rate of 640 Gbit/s, the fastest DEMUX reported so far. The advantage of fiber based switching devices is their potential for ultrafast switching due to the fast non-resonant nonlinearity of the fiber. The main drawback of these devices stems from the small optical nonlinearity of glass. For an optical switch, the product of control power times the fiber length of conventional fiber must be about 1 W km. In recent years, however, new fibers have been developed called "highly non-linear fibers" (HNLF). At present, the product of control power times fibre length of HNLF needs only to be about 0.1 W km mainly because of the smaller effective area of the HNLF. Chapter 6 ("Optical signal processing using nonlinear fibers", by Watanabe) reports on all-optical signal processing using HNLF for demultiplexing and other ap-

plications. Another type of new optical fiber is the photonic crystal fiber [25]. Optical signal processing based on photonic crystal fiber is not explicitly reported in this book.

Another class of optical switching devices uses the high resonant nonlinearity in active semiconductor structures. Chapter 5 ("High-speed optical signal processing using semiconductor optical amplifiers", by Schubert et al.) reports on optical gating devices based on XPM and FWM in a semiconductor optical amplifier (SOA). Examples of XPM based optical gates include the SOA in a Mach-Zehnder interferometer (SOA-MZI), the SOA in a polarization discriminating switch (SOA-UNI), and the SOA in a Sagnac interferometer (SLALOM). These devices have been used as DEMUX in several high-speed transmission experiments. Examples are the SOA-MZI DEMUX in transmission experiments at bit rates of up to 320 Gbit/s [26,27], and the SLALOM DEMUX in a 640-Gbit/s demultiplexing experiment, where 8 WDM channels, each carrying an 80-Gbit/s TDM data signal, were simultaneously demultiplexed in the time domain to 8 further WDM channels, each carrying a 10-Gbit/s TDM data signal [28]. The advantage of the SOA based switching devices is their small size and their low optical power requirement for all-optical switching. Moreover, these devices can be realized as photonic integrated circuits.

SOA- and fiber-based optical gates use all-optical switching. An optical signal controls the gate, which switches an optical data signal. Another optical gate used in many high-speed transmission experiments is the electroabsorption modulator (EAM). In this device an electrical control signal controls the gate that switches the optical data signal. This switch has been used for demultiplexing in many transmission experiments as described in chapter 13 ("Application of electroabsorption modulators for high-speed transmission systems", by Lach et al.). Recently, an EAM was monolithically integrated with a photodiode and an electrical signal from the photodiode drove the EAM directly [29, 30].

The demultiplexers described above are capable of selecting only one TDM channel of the multiplexed data signal (single channel output operation). Multiple channel output operation can be achieved by a serial-parallel configuration of several of these switches. An example is reported in [31] and discussed in chapter 15 ("Ultrafast optical technologies for large-capacity TDM/WDM photonic networks", by Morioka). This chapter also reports on the realization of optical switches that provide a multiple channel output directly in a single device. The reported examples utilize XPM-assisted chirp compensation in an optical fiber or FWM by employing linearly chirped square control pulses to generate different frequency components corresponding to independent TDM channels.

SOA- and EAM-based optical switching devices operate well at data rates of up to 160 Gbit/s. Their performance worsens considerably at higher data rates. Chapter 16 ("New optical device technologies for ultrafast OTDM systems", by Sakurai and Kobayashi) reports on investigations into new optical device technologies, which will enable faster switching devices to be realized for future ultrafast OTDM transmission systems.

Clock recovery or timing extraction from a transmitted data signal is another key function in an OTDM receiver and in other subsystems such as add-drop multiplexers and 3R-regenerators. Several timing extraction techniques have been developed including phase-locked loops (PLL), the injection locking of pulse sources, and resonant oscillator circuits [4,5]. At data rates of 160 Gbit/s and beyond, clock recovery was most successfully achieved by using PLL configurations with an optical or opto-

electrical phase comparator. Chapters 5 ("High-speed optical signal processing using semiconductor optical amplifiers", by Schubert et al.) and 15 ("Ultrafast optical technologies for large-capacity TDM/WDM photonic networks", by Morioka) report on the application of SOAs as optical phase comparators using either FWM or XPM in an SOA and chapter 13 ("Application of electroabsorption modulators for high-speed transmission systems", by Lach et al.) reports on the application of EAMs as optoelectrical phase comparators in a clock recovery circuit. SOA-based and EAM-based clock recovery devices have been operated at up to 400 [32] and 320 Gbit/s [33], respectively.

Many transmission experiments were also performed without recovering the clock signal from the multiplexed data signal, because an appropriate clock recovery device was unavailable. Two alternative approaches were used. A clock signal was generated at the transmitter and transmitted together with the data signal over the fiber at a separate wavelength ("clock transmitted"), or the multiplexer at the transmitter end was adjusted for slightly different pulse amplitudes ("clock modulation") such that a simple photo detector was able to detect the clock signal at the receiver end.

In the OTDM experiments reported to date, the O/E receivers were operated at up to 40 Gbit/s. However, in laboratory experiments O/E receivers have already operated at data rates of up to about 80 Gbit/s [9]. Chapter 7 ("Ultrafast photodetectors and receivers", by Bach) reports on ultrafast photodetectors and receivers. It is expected that ETDM transmission systems will soon be available for data rates up to 100 Gbit/s. This will most likely increase the base rate of OTDM systems from 40 to 100 Gbit/s.

5. Transmission Fiber, Compensation of Chromatic Dispersion and Polarization Mode Dispersion, 2R/3R-Regeneration

A data signal is degraded along a transmission line by attenuation, fiber non-linearity, chromatic dispersion (CD) and the polarization mode dispersion (PMD) of the fiber, and the accumulation of noise generated in the amplifier stages. These impairments can be partly compensated for, depending on the type of transmission fiber used.

For a 160-Gbit/s system, it is necessary to compensate not only for chromatic dispersion (D or β_2) at the center wavelength of the pulse but also for the dispersion slope ($dD/d\lambda$ or β_3). The dispersion slope produces oscillations near the trailing edge of the data pulse even if the center wavelength of the pulse is adjusted to the zero-dispersion point of the path-averaged dispersion. Currently, the most mature dispersion compensation technique is based on dispersion compensating fibres (DCF), which compensate simultaneously for both D and $dD/d\lambda$. DCF, also sometimes known as high-slope dispersion compensating fiber (HS-DCF), has become an essential optical component supporting high-speed large capacity optical transmission. DCF has further evolved into dispersion-managed optical fiber transmission lines. Chapter 9 ("Optical fibers and fiber dispersion compensators for high-speed optical communication", by Nishimura) reports on DCF and dispersion-managed optical transmission lines as well as on advanced optical fiber such as ultra-low loss or ultra-low nonlinearity fiber and various types of dispersion-modified fiber.

Dispersion compensation using DCF is insufficient for very high bit rate transmission (640 Gbit/s and beyond) in most fibers. Higher order dispersion terms (β_4) have to be taken into account. This is dealt with in chapter 11 ("Higher-order dispersion compensation using phase modulators", by Pelusi and Suzuki). This chapter focuses

on the use of a phase modulation technique that has been effectively employed in the fastest OTDM fiber transmission experiments using OOK modulation format reported to date [see chapter 14 ("Ultrafast OTDM transmission using novel fiber devices for pulse compression, shaping, and demultiplexing", by Yamamoto and Nakazawa)]).

Various types of transmission fiber and their associated DCF have been investigated for high-speed data transmission. Examples are standard single-mode fiber (SMF, $D \cong 17$ ps/km/nm at $\lambda = 1550$ nm), dispersion shifted fiber (DSF, $D \cong 0.1$ ps/km/nm), and various types of non-zero dispersion shifted fiber (NZDSF, $D \cong 4$–8 ps/km/nm), e.g., TrueWave^{TM}, LEAF^{TM} and TeraLight^{TM}. Additionally, there are several types of dispersion-managed fiber (DMF) such as "TeraLight^{TM}-Reverse TeraLight^{TM}", SMF-reverse dispersion fiber (SMF-RDF) and "Ultrawave^{TM} Fiber" (SLA-IDF). The DMF represents a pair of transmission fibers, which together compensate for D and $dD/d\lambda$ over a wide wavelength range. For example Ultrawave^{TM} Fiber comprises Super Large Area fiber (SLA, $D \cong 20$ ps/km/nm) and Inverse Dispersion Fiber (IDF, $D \cong -44$ ps/km/nm).

The tolerances as regards residual dispersion or residual DCF length are particularly crucial for high-speed systems. For instance, for a data rate of 160 Gbit/s over 160 km of SMF, the 3 dB tolerance (an increase in the pulse width by a factor of two) is $\pm$ 1.2 ps/nm. This corresponds to a DCF fiber length tolerance of $\pm$ 12 m or an SMF fiber length tolerance of $\pm$ 75 m. To maintain such small tolerances over a large environmental temperature range requires automatic dispersion compensation in addition to the DCF fiber. Various tunable dispersion compensators have been proposed [34–37]. In particular, the chirped fiber Bragg grating (FBG) is a key device for tunable dispersion compensation. Chapter 10 ("Fiber Bragg gratings for dispersion compensation in optical communication systems", by Sumetsky and Eggleton) presents an overview of FBG fabrication principles and applications with emphasis on the chirped FBG used for dispersion compensation in high-speed optical communication systems. An example of a tunable dispersion compensator is also discussed in chapter 15 ("Ultrafast optical technologies for large-capacity TDM/WDM photonic networks", by Morioka).

High-speed transmission experiments are commonly performed in the quasi-linear (pseudo-linear) transmission regime, where the nonlinear length is much greater than the dispersion length [e.g., 38]. A high local dispersion is advantageous for this transmission regime, provided that the path-averaged dispersion and dispersion slope are close to zero. The short pulses of the data signal disperse very quickly in the fiber, spreading into many adjacent timeslots before the original pulse sequence is restored by dispersion compensation. Therefore, the peak power of the pulses is low for most of the path along the fiber. Consequently, fibers with high dispersion D are most appropriate for high-speed transmission. For example, with 160 Gbit/s data transmission, impressive results with transmission spans of up to 2,000 km have been obtained using NZDSF [39]. However, 160 Gbit/s data transmission over the Ultrawave^{TM} Fiber with its high local dispersion and low non-linearity achieved a transmission distance of more than 4,000 km [40]. In these experiments, intra-channel FWM is the main degradation factor as regards data signals with high optical powers.

PMD is also a severe limitation with respect to high bit rate data transmission. PMD is caused by a slight birefringence of the fiber and of other components in the transmission link. Based on the example cited above, a PMD value of less than 0.07 ps/$\sqrt{\text{km}}$ is needed to realize a low penalty 160 Gbit/s transmission over a 160-km fiber link. Modern fiber such as Ultrawave^{TM} Fiber has a PMD value of less than 0.05

Table 1. Examples of ultra-high-speed optical transmission experiments.

Date	TDM bit rate (Gbit/s)	WDM channel	Modulation format	Transmission length (km, fiber)	Span length (km, repeater)	Pulse source	Demux	Clock Recovery	Institute	Ref.
03/95	160	1	OOK, AP	200 DSF	25, EDFA	ML-FRL+PuC	POL+NOLM	clock modulation	NTT	46
05/95	200	1	OOK, SP	100 DSF	20, 40,EDFA	SC-pulse	FWM in Fiber	PLL, FWM in SOA	NTT	47
05/96	400	1	OOK,SP	40 SMF	unrepeatered	SC-pulse	FWM in Fiber	PLL, FWM in SOA	NTT	48
09/97	200	7	OOK, SP	50 DSF	unrepeatered	SC-pulse	FWM in Fiber	PLL, FWM in SOA	NTT	52
04/98	640	1	OOK, SP	60 SMF	unrepeatered	ML-FRL+PuC	NOLM	clock modulation	NTT	49
05/99	160	19	OOK, SP	40 DSF	unrepeatered	SC-pulse	FWM in Fiber	PLL, FWM in SOA	NTT	53
09/99	160	1	OOK, AP	300 TW	100, EDFA	CW+Mod+PuC	2 EAM	resonant-oscillator	Lucent	61
03/00	320	1	OOK, AP	200 TW	100, Raman	CW + Mod	POL+2 EAM	resonant-oscillator	Lucent	38
09/00	160	1	OOK, SP	160 SMF	unrepeatered	ML-LD	SOA-MZI	transmitted	HHI	54
11/00	1280	1	OOK, AP	70 SMF +RDF	unrepeatered	ML-FRL+PuC	POL+NOLM	transmitted	NTT	51
03/01	160	6	OOK, AP	400 TW	100, Raman	SC-pulse	2 EAM	resonant-oscillator	Lucent	67
03/01	160	1	OOK, SP	116 SMF, field trial	unrepeatered	ML-LD	SOA-UNI	transmitted	HHI	55
09/01	160	1	OOK, SP	200 TW-RS,LEAF	unrepeatered	CW+Mod+PuC	3 EAM	resonant-oscillator	Agere	62
08/03	160	4	OOK, AP, CS-RZ	225 NZ-DSF	75, EDFA	CW + Mod	POL+ 2 EAM	resonant-oscillator	KDDI	71
09/03	160	1	OOK, SP,CS-RZ	640 SMF	80, Raman	CW + Mod	2 EAM	PLL	OKI	23
09/03	160	8	OOK, AP, CS-RZ	85 TeraLight-Ultra	unrepeatered	CW + Mod	1 EAM +POL	resonant-oscillator	Alcatel	69
09/03	160 +7%FEC	7	OOK, AP, CS-RZ	600 SMF	100, Raman	CW + Mod	1 EAM +POL	transmitted	Alcatel	70
09/03	160	8	OOK, SP	140 SMF	unrepeatered	SC-pulse	SOA-MZI	transmitted	FESTA /OKI/NEC	57
10/03	160	1	DPSK, SP	410, SLA+IDF	80, EDFA	ML-LD	1 EAM	EO-PLL, EAM	HHI	75
11/03	160+7%FEC	6	DPSK, AP	2000 TW-RS	100, Raman	CW + Mod	1 EAM,40Gb/s	clock modulation	Lucent	39
02/04	160	1	OOK, SP	160, SMF+RDF	80, Raman	SC-pulse	all channel	transmitted	NTT/ Stanford Univ.	22
07/04	160	1	DPSK, SP	200 SMF,field trial	50, EDFA	CW+Mod+PuC	2 EAM,40Gb/s	EO-PLL, EAM	KDDI/ NICT	77
09/04	160	1	OOK, SP	275 SMF, field trial	69, EDFA	solid state	FWM in SOA	EO-PLL, EAM	Siemens/ BT	58
09/04	160+7%FEC	8	OOK, AP, CS-RZ	430 SMF, field trial	71, EDFA	CW + Mod	1 EAM +Pol	resonant-oscillator	Alcatel/ FT/ DT	45
09/04	320	10	OOK, SP	40, SMF	unrepeatered	SC-pulse	SOA-MZI	transmitted	FESTA /OKI/NEC	26
09/04	640	1	DPSK, AP	160 SLA+IDF	80, EDFA	ML.-FRL	POL+NOLM	EO-PLL, EAM	HHI / Fujitsu	80
09/05	160+7%FEC	1	DPSK, AP	4300 SLA+IDF	80, Raman	ML.-LD	1 EAM,40Gb/s	EO-PLL, EAM	HHI/ Lucent(G)	40
09/05	640	1	DQPSK, AP	480 SLA+IDF	80, EDFA	ML.-LD	POL+ 1 EAM	EO-PLL, EAM	HHI	84
02/06	1280	1	DQPSK, AP	240 SLA+IDF	80, EDFA	solid state	POL+NOLM	EO-PLL, EAM	HHI/Fujitsu	85
02/06	2400+7%FEC	1	DQPSK, AP	160 SLA+IDF	80, EDFA	solid state	POL+NOLM	clock modul.+PLL	HHI/Fujitsu	85

ps/$\sqrt{\text{km}}$. On the other hand, older installed fiber generally has a larger PMD value. Unlike CD, PMD is much more difficult to compensate for because it changes greatly with time and wavelength in a non-deterministic way. Therefore, automatic (adaptive) PMD compensation is required. Chapter 12 ("PMD-compensation techniques", by Rosenfeldt and Brinkmeyer) deals with PMD compensation techniques. Adaptive PMD compensation has been demonstrated for data rates of up to 160 Gbit/s [41–45]. In most ultrahigh bit rate transmission experiments, PMD (first order) was compensated for by manually adjusting the polarization of the data signal at the transmission link input.

For advanced transmission systems, 3R-regeneration (re-amplification, re-shaping, re-timing) is needed to reduce the transmission impairments, which are associated with waveform distortions caused by fiber transmission as well as with noise and jitter accumulation. There has been little experimental work on this topic as regards high bit rate data transmission. Chapter 6 ("Optical signal processing using nonlinear fibers", by Watanabe) reports on a 160-Gbit/s 3R-regenerator experiment [19]. Chapter 8 ("Optical nonlinearities in semiconductor optical amplifier and electro-absorption modulator: their applications to all-optical regeneration", by Usami and Nishimura) provides some references to 2R and 3R regenerator experiments for data rates below 160 Gbit/s.

6. Transmission Experiments

In this review we focus on the recent developments with respect to OTDM transmission experiments as early transmission experiments have been discussed in previous review articles [3–5]. Table 1 is a summary of important and recent high bit rate transmission experiments at TDM bit rates of 160 Gbit/s and beyond. Many of the pioneering OTDM-transmission experiments were performed by NTT and are described in chapter 15 ("Ultrafast optical technologies for large-capacity TDM/WDM photonic networks", by Morioka). Examples include 160 Gbit/s soliton transmission over 200 km DSF [46], 200 Gbit/s transmission over 100 km DSF [47], 400 Gbit/s over 40 km SMF [48], 640 Gbit/s over 60 km and 92 km SMF [49,50] and finally 1.28 Tbit/s over 70 km DMF (SMF+RDF) [51]. In addition to these single wavelength channel transmission experiments, chapter 15 ("Ultrafast optical technologies for large-capacity TDM/WDM photonic networks", by Morioka) also describes pioneering OTDM/WDM experiments performed by NTT such as 1.4 Tbit/s (200 Gbit/s $\times$ 7 λ) over 50 km DSF [52] and 3 Tbit/s (160 Gbit/s $\times$ 19 λ) over 40 km DSF [53]. These experiments combine ultrafast OTDM and ultra-wideband WDM technologies.

In these experiments, the terminal equipment mainly comprised fiber devices. The pulse source in the transmitter was either a mode-locked fiber ring laser (ML-FRL) followed by an optical pulse compressor (PuC) or a pulse source based on supercontinuum generation (SC-pulse). The demultiplexer in the OTDM-receiver was an optical gate based either on a nonlinear optical loop mirror (NOLM) or on four-wave-mixing (FWM) in fiber. An exception was the optical clock recovery device, which comprised a PLL with a phase comparator based on FWM in a semiconductor optical amplifier (SOA). EDFAs were used as in-line amplifiers.

The NTT work represents investigations on the physical limits of high-speed fiber transmission and the search for appropriate data generation, transmission and demultiplexing techniques to extend these limits. An extraordinary 1.28 Tbit/s (640 Gbit/s $\times$

2 polarization-division multiplexing) single wavelength channel transmission experiment is described in detail in chapter 14 ("Ultrafast OTDM transmission using novel fiber devices for pulse compression, shaping, and demultiplexing", by Yamamoto and Nakazawa). This chapter covers the adiabatic soliton compression technique, which compresses the optical pulses of an ML-FRL, a technique for eliminating the pedestals of the compressed optical pulses, and an all-optical demultiplexing technique employing a NOLM with very small walk-off.

An alternative to fiber-based optical signal processing is the employment of semiconductor devices for optical signal processing in the transmitter and receiver of the OTDM system. In particular, the SOA has long been considered a key device for optical signal processing. Chapter 5 ("High-speed optical signal processing using semiconductor optical amplifiers", by Schubert et al.) describes the technology of SOA-based devices such as optical gates, optical clock recovery devices and optical add-drop multiplexers. These devices have been used in several transmission experiments [54–58,26,12,22]. Examples of single wavelength channel transmission include unrepeatered 160 Gbit/s transmission over 160 km SMF using a hybrid SOA-MZI DEMUX [54], the first 160-Gbit/s field trial involving unrepeatered transmission over 116 km field-installed SMF using an SOA-UNI DEMUX [55] and a 160 Gbit/s field trial over various link lengths of installed fiber of up to 275 km SMF using a DEMUX based on FWM in a SOA [58,12]. The latter field experiment is of particular interest because it also includes a 160 Gbit/s add-drop node based on gain-transparent operation of a SOA [see chapter 5 ("High-speed optical signal processing using semiconductor optical amplifiers", by Schubert et al.)]. This is the first OTDM networking experiment using deployed fiber. Also of particular importance is the first 160 Gbit/s OTDM transmission experiment with all-channel independent modulation and all-channel simultaneous demultiplexing achieved by using a multiplexer and a demultiplexer based on periodically poled lithium niobate and SOA hybrid integrated planar lightwave circuits [22]. This transmission experiment is described in detail in chapter 15 ("Ultrafast optical technologies for large-capacity TDM/WDM photonic networks", by Morioka). A hybrid-integrated SOA-MZI DEMUX was operated in two OTDM/WDM transmission experiments, namely, 1.28 Tbit/s (160 Gbit/s $\times$ 8λ) unrepeatered transmission over 140 km SMF [57] and 3.2 Tbit/s (320 Gbit/s $\times$ 10λ) transmission over 40 km SMF [26]. In these experiments the spectral efficiencies were 0.4 and 0.8 bit/s/Hz, respectively.

At present, the SOA based optical gate is probably not the most popular choice for demultiplexing applications in 160 Gbit/s transmission systems. Another semiconductor device, the EAM, has been developed into a very effective component for optical signal processing. In pioneering experiments, British Telecom (BT) demonstrated the application of the EAM for OTDM data generation and demultiplexing [59,60]. Lucent Technologies reported the first 160 Gbit/s transmission experiment, which used the EAM as a key device in the transmitter and the receiver [61]. This investigation also stimulated similar experiments in many other laboratories [62–65], because 160 Gbit/s transmission became viable without such sophisticated devices for demultiplexing as interferometric optical gates or FWM configurations based on SOAs or fibers, and without sophisticated optical pulse sources. The EAM was used as an optical gate in the demultiplexer, as a basic element in the clock recovery circuit and as a device for optical pulse generation (CW + Mod). Moreover, the EAM-based demultiplexer is polarization insensitive, which is difficult to achieve with the fiber-

based and SOA-based demultiplexers. Also, the EAM-based demultiplexer does not need an optical pulse source to operate the optical gate. The simpler technology of the EAM-based OTDM-system also stimulated 320 Gbit/s transmission experiments using AP-multiplexing [66,38] and several $N\times$ 160 Gbit/s OTDM/WDM transmission experiments [67–71,45]. Chapter 13 ("Application of electroabsorption modulators for high-speed transmission systems", by Lach et al.) focuses on OTDM transmission technology based on EAMs. This chapter reviews the various applications of the EAM in the transmitter and receiver in ultra-high speed OTDM-transmission systems and also presents the results of single channel and WDM/OTDM fiber transmission experiments.

In the experiments mentioned above, the modulation format was on-off-keying (OOK). Moreover, in most of these experiments the relative phase of adjacent pulses (RZ-signals) was arbitrary, because in general no effort was made in these experiments to adjust and stabilize the delay line multiplexers for a well-defined relative phase of the adjacent pulses. However, the controllability of the optical phase alignment between adjacent bits is an important feature of an OTDM system [72]. The effect of a well-defined relative phase of adjacent data pulses in the multiplexed data signal is expected to increase the tolerance of the transmission system with respect to CD and fiber nonlinearity and it will increase the spectral efficiency. Techniques for realizing optical phase alignment have been introduced [73,74] and several OTDM and OTDM/WDM transmission experiments have been performed using such formats as "carrier-suppressed return-to-zero (CS-RZ)", in which the optical pulses in adjacent bit slots have a relative phase shift of π [23,69–71,45].

Recently, several OTDM-transmission experiments have been performed using modulation format differential phase shift keying (DPSK) [75–80, 39,40]. In combination with balanced detection, 160 Gbit/s DPSK transmission provided a system performance that was more than 3 dB better than transmission with the OOK modulation format [76]. The increased system margin can be used to extend the transmission length or to reduce the optical power requirements. On the other hand, additional components are needed in the transmitter and receiver. In particular, the DPSK demodulator in the receiver needs to be actively matched to the transmitter wavelength, which increases the system complexity. Nevertheless, the improvement in the system performance is significant and worth the additional system cost and complexity. The increased system margin also made it possible to realize a 640-Gbit/s DPSK, AP transmission over a 160 km dispersion managed fiber link [80].

In the past, many high-bit-rate transmission experiments were "proof of feasibility" experiments. It was sufficient simply to obtain a system that was stable for the few minutes needed to perform BER measurements. Recently, it was also shown that OTDM transmission systems can have long-term stability [78,79]. In a 160-Gbit/s DPSK transmission over a 320-km fiber link, BER measurements revealed, that the system operated without any error for more than 5 hours. This corresponds to a BER of about 10^{-15}. The first errors were detected after 5 hours and these were caused by a slight drifting of some parts of the system with increases in the environmental temperature. There were 32 errors within 10 hours. After 10 hours the system was readjusted and error-free performance was again obtained. No PMD compensator was required in this experiment because of the high quality of the Ultrawave^{TM} Fiber used. Similar results were also obtained using a 334-km SMF fiber link including a PMD mitigation scheme [79]. In both experiments, the transmission system comprised a

semiconductor mode-locked laser (ML-LD) in the transmitter and two EAMs in the demultiplexer (one in the optical gate and one in the clock recovery). If this system is equipped with an automatic stabilization circuit and FEC, it can probably be operated error free for many years. The system has a stability appropriate for applications in a deployed transmission link.

Some further recent transmission experiments concern DQPSK transmission with data rates of 160 Gbit/s and higher [82-85]. DQPSK transmission provides a bit rate that is twice the symbol bit rate. Based on 40 Gbit/s ETDM technology, the application of DQPSK provides 80 Gbit/s data transmission. In [82,83] this was further combined with polarization-division multiplexing (AP multiplexing) to generate a 160-Gbit/s data signal. In this experiment, 40 WDM channels, each carrying a 160 Gbit/s data signal generated in this way, were transmitted over a 324-km SMF fiber link. The system was operated above the FEC limit. This corresponds to a 5.94-Tbit/s error-free transmission conditional on the use of FEC. A spectral efficiency of 1.6 bit/s/Hz was obtained. In another experiment, the 160-Gbit/s OTDM-SP-multiplexing transmission technology was upgraded to 640 Gbit/s by applying the modulation format DQPSK and polarization-division multiplexing (AP multiplexing). A 640-Gbit/s DQPSK data signal was transmitted over 480 km DMF (SLA-IDF) error-free without FEC [84].

Most recently, DQPSK transmission with AP multiplexing was also realized at 1.28 Tbit/s over 240 km and 2.56 Tbit/s over 160 km fiber link [85]. For 1.28 Tbit/s, error-free (BER $< 10^{-9}$) transmission was obtained for all tributaries of the 1.28 Tbit/s data signal. For 2.56 Tbit/s transmission, the system performed nearly error-free (BER $\approx 10^{-9}$) in the back-to-back configuration and revealed BER-values $\leq 10^{-5}$ after 160 km transmission. BER values of less than 10^{-4} result in an effective BER $< 10^{-12}$ if standard FEC (assuming a 7% overhead) is used. This FEC would reduce the payload to 2.4 Tbit/s.

References

1. K. Fukuchi, T. Kasamatsu, M. Morie, R. Ohhira, T. Ito, K. Sekiya, D. Ogasahara, and T. Ono, "10.92 Tb/s (273 × 40 Gb/s) triple-band/ultra-dense WDM optical-repeatered transmission experiment" in Proc. Optical Fiber Communication Conference, OFC 2001, postdeadline papers, PD 24 (2001).
2. S. Biego, Y. Frignac, G. Charlet, W. Idler, S. Borne, H. Gross, R. Dischler, W. Poehlmann, P. Tran, C. Simonneau, D. Bayart, G. Veith, A. Jourdan, J.-P. Hamaide, "10.2 Tbit/s (256 × 42.7 Gbit/s PDM/WDM) transmission over 100 km TeraLight fiber with 1.28 bit/s/Hz spectral efficiency" in Proc. Optical Fiber Communication Conference, OFC 2001, postdeadline papers, PD 25 (2001).
3. S. Kawanishi, "Ultrahigh-speed optical time-division-multiplexed transmission technology based on optical signal processing", IEEE J. Quantum Electron. **34**, 2064–2079 (1998).
4. M. Saruwatari, "All-optical signal processing for Tera bit/s optical transmission", IEEE J. Select Topics Quantum Electron. **6**, 1363–1374 (2000).
5. M. Saruwatari, "All-optical time-division multiplexing technology" in *Fiber Optic Communication Devices*, edited by N. Grote, H. Venghaus (Springer-Verlag, Berlin, 2001).
6. A. Joseph, D. Coolbaugh, D. Harame, G. Freeman, S. Subbanna, M. Doherty, J. Dunn, C. Dickey, D. Greenberg, R. Groves, M. Meghelli, A. Rylyakov, M. Sorna, O. Schreiber, D. Herman, and T. Tanji, "0.13 μm 210 GHz f_T SiGe HBTs—expanding the horizons of

SiGe BiCMOS", International Solid-State Circuits Conference, ISSCC, Digest of Technical papers, pp. 180–181 (2002).

7. Y. Yu, R. Lewen, S. Irmscher, U. Westergren, L. Thylen, U. Eriksson, and W.S. Lee, "80 Gb/s ETDM Transmitter with a Traveling-Wave Electroabsorption Modulator", in Proc. Optical Fiber Communication Conference, OFC 2005, Paper OWE1 (2005).
8. H.-G. Bach, A. Beling, G.G. Mekonnen, R. Kunkel, D. Schmidt, W. Ebert, A. Seeger, M. Stollberg, and W. Schlaak, "InP-Based Waveguide-Integrated Photodetector with 100 GHz Bandwidth", IEEE J. Select. Topics on Quantum Electron. **10** (4), 668–672 (2004).
9. K. Schuh, B. Junginger, E. Lach, A. Klekamp, E. Schlag, "85.4 Gbit/s ETDM receiver with full rate electronic clock recovery", in Proc. European Conference on Optical Communication, ECOC 2004, PDP Th4.1.1 (2004).
10. O. Kamatani and S. Kawanishi, "Add/drop operation for 100 Gbit/s optical signal based on optical wavelength conversion by four-wave mixing", Electron. Lett. **32**, 911–913 (1996).
11. C. Schubert, C. Schmidt, S. Ferber, R. Ludwig, and H.G. Weber, "Error-free all-optical add-drop multiplexing at 160 Gbit/s", Electron. Lett. **39**, 1074–1076 (2003).
12. J.P. Turkiewicz, E. Tangdiongga, G. Lehmann, H. Rohde, W. Schairer, Y.R. Zhou, E.S.R. Sikora, A. Lord, D.B. Payne, G.-D. Khoe, and H. de Waardt, "160 Gbit/s OTDM networking using deployed fiber", J. Lightwave Technol. **23**, 225–235 (2005).
13. H.F. Chou, J.E. Bowers, and D.J. Blumenthal, "Compact 160-Gb/s Add-Drop Multiplexing with a 40-Gb/s Base-Rate", Optical Fiber Communication Conf., 2004, PDP28 (2004).
14. S. Nakamura, Y. Ueno, and K. Tajima, "168-Gb/s all-optical wavelength conversion with a symmetric-Mach-Zehnder-type switch", Photon. Technol. Lett. **13**, 1091–1093 (2001).
15. J. Leuthold, C. Joyner, B. Mikkelsen, G. Raybon, J. Pleumeekers, B. Miller, K. Dreyer, and C. Burrus, "100 Gbit/s all-optical wavelength conversion with integrated SOA delayed-interference configuration", Electron. Lett. **36**, 1129–1130 (2000).
16. J. Hansryd, P.A. Andrekson, M. Westlund, J. Li, and P.-O. Hedekvist, "Fiber-based optical parametric amplifiers and their applications", IEEE J. Select. Topics Quantum Electron. **8**, 506–520 (2002).
17. F. Futami, R. Okabe, Y. Takita, and S. Watanabe, "Transparent wavelength conversion at up to 160 Gb/s by using supercontinuum generation in a nonlinear fiber", Proc. Optical Amplifiers and Applications, OAA 2003 at Otaru, Japan, Paper MD07 (2003).
18. S. Ferber, R. Ludwig, F. Futami, S. Watanabe, C. Boerner, C. Schmidt-Langhorst, L. Molle, K. Habel, M. Rohde, and H.G.Weber, "160 Gbit/s regenerating conversion node", in Proc. Optical Fiber Communication Conference, OFC 2004, Los Angeles, CA, USA, paper ThT2 (2004).
19. S. Watanabe, R. Ludwig, F. Futami, C. Schubert, S. Ferber, C. Boerner, C. Schmidt-Langhorst, J. Berger, and H.G. Weber, "Ultrafast all-optical 3R-regeneration", IEICE Trans. Electron. **E87-C** (7), 1114–1118 (2004).
20. P.V. Mamyshev, "All-optical data regeneration based on self-phase modulation effect", in Proc. European Conference on Optical Communications, ECOC 1998, Madrid, Spain, Volume 1, pp. 475–476 (1998).
21. T. Ohara, H. Takara, I. Shake, K. Mori, S. Kawanishi, S. Mino, T. Yamada, M. Ishii, T. Kitoh. T. Kitagawa, K.R. Parameswaran, and M.M. Fejer, "160 Gbit/s optical-time-division multiplexing with PPLN hybrid integrated planar lightwave circuit", IEEE Photon. Technol. Lett. **15**, 302–304 (2003).

22. T. Ohara, H. Takara, I. Shake, K. Mori, K. Sato, S. Kawanishi, S. Mino, T. Yamada, M. Ishii, I. Ogawa, T. Kitoh, K. Magari, M. Okamoto, R.V. Roussev, J.R. Kurz, K.R. Parameswaran, and M.M. Fejer, "160-Gb/s OTDM transmission using integrated all-optical MUX/DEMUX with all-channel modulation and demultiplexing", IEEE Photon. Technol. Lett. **16**, 650–652 (2004).
23. H. Murai, K. Masatoshi, H. Tsuji, and K. Fujii, "Single Channel 160 Gbit/s Carrier-Suppressed RZ Transmission over 640 km with EA Modulator based OTDM Module", ECOC 2003, paper Mo.3.6.4, Rimini.
24. K.J. Blow, N.J. Doran, and B.P. Nelson, "Demonstration of the nonlinear fibre loop mirror as an ultrafast all-optical demultiplexer", Electron. Lett. **26**, 962–963 (1990).
25. A. Bjarklev, J. Broeng, and A.S. Bjarklev, *Photonic Crystal Fibers* (Kluwer Academic Publishers, Dordrecht, The Netherlands, 2003).
26. A. Suzuki, X. Wang, Y. Ogawa, and S. Nakamura, "10 × 320 Gbit/s (3.2 Tbit/s) DWDM/OTDM transmission by semiconductor based devices", Proc. ECOC 2004, paper Th4.1.7.
27. K. Tajima, S. Nakamura, and A. Furukawa, "Hybrid-integrated symmetric Mach-Zehnder all-optical switches and ultrafast signal processing" IEICE Trans. Electron. **E87-C** (7), 1119–1125 (2004).
28. S. Diez, R. Ludwig, and H.G. Weber, "All-optical switch for TDM and WDM/TDM systems demonstrated in a 640 Gbit/s demultiplexing experiment", Electron. Lett. **34**, 803 (1998).
29. S. Kodama, T. Yoshimatsu, and H. Ito, "320 Gbit/s error-free demultiplexing using ultrafast optical gate monolithically integrating a photodiode and electroabsorption modulator", Electron. Lett. **39** (17), 1269–1270 (2003).
30. S. Kodama, T. Yoshimatsu, and H. Ito, "500-Gbit/s demultiplexing operation of monolithic PD-EAM gate", postdeadline paper Th4.2.8, ECOC 2003, Rimini.
31. I. Shake, H. Takara, K. Uchiyama, I. Ogawa, T. Kitoh, T. Kitagawa, M. Okamoto, K. Magari, Y. Suzuki, and T. Morioka, "160 Gbit/s full optical time-division demultiplexing using FWM of SOA-array integrated on PLC", Electron Lett. **38**, 37–38 (2002).
32. O. Kamatani and S. Kawanishi, "Prescaled Timing extraction from 400 Gbit/s optical signal using a phase lock loop based on four-wave mixing", IEEE Photon. Technol. Lett. **8**, 1094–1096 (1996).
33. C. Boerner, V. Marembert, S. Ferber, C. Schubert, C. Schmidt-Langhorst, R. Ludwig, and H.G. Weber, "320 Gbit/s clock recovery with electro-optical PLL using a bidirectionally operated electroabsorption modulator as phase comparator" in Proc. Optical Fiber Communication Conference, OFC 2005, paper OTuO3 (2005).
34. B. J. Eggleton, B. Mikkelsen, G. Raybon, A. Ahuja, J.A. Rogers, P.S. Westbrook, T.N. Nielsen, S. Stulz, and K. Dreyer, "Tunable dispersion compensation in a 160 Gb/s TDM system by voltage controlled chirped fiber Bragg grating" IEEE Photon.Technol. Lett. **12**, 1022–1024 (2000).
35. C.K. Madsen, "Integrated waveguide allpass filter tunable dispersion compensator", OFC' 2002, TuT1.
36. T. Inui, T. Komukai, M. Nakazawa, K. Suzuki, K.R. Tamura, K. Uchiyama, and T. Morioka, "Adaptive dispersion slope equalizer using a nonlinearly chirped fiber Bragg grating pair with a novel dispersion detection technique", IEEE Photon. Technol. Lett. **14**, 549–551 (2002).
37. S. Wakabayashi, A. Baba, H. Moriya, X. Wang, T. Hasegawa, and A. Suzuki, "Tunable dispersion and dispersion slope compensator based on two twin chirped FBGs with temperature gradient for 160 Gbit/s transmission." IEICE Trans. Electron. **E87-C**, 1100–1105 (2004).

38. B. Mikkelsen, G. Raybon, R.-J. Essiambre, A.J. Stentz, T.N. Nielsen, D.W. Peckham, L. Hsu, L. Gruner-Nielsen, K. Dreyer, and J.E. Johnson, "320 Gbit/s single-channel pseudolinear transmission over 200 km nonzero-dispersion fiber", IEEE Photon. Technol. Lett. **12**, 1400–1402 (2000).

39. A.H. Gnauck, G. Raybon, P.G. Bernasconi, J. Leuthold, C.R. Doerr, and L.W. Stulz, "1 Tb/s 6×170.6 Gb/s) transmission over 2000 km NZDF using OTDM and RZ-DPSK", IEEE Photon. Technol. Lett. **15** (11), 1618–1620 (2003).

40. S. Weisser, S. Ferber, L. Raddatz, R. Ludwig, A. Benz, C. Boerner, H.G. Weber, "Single- and Alternating Polarization 170 Gbit/s Transmission up to 4000 km using Dispersion-Managed Fiber and All-Raman Amplification", IEEE Photon. Technol. Lett. **18** (12), 1320–1322 (2006).

41. M. Westlund, H. Sunnerud, J. Li, J. Hansryd, M. Karlsson, P.O. Hedekvist, and P.A. Andrekson, "Long-term automatic PMD compensation for 160 Gbit/s RZ transmission", Electron. Lett. **38**, 982–983 (2002).

42. T. Miyazaki, M. Daikoku, I. Morita, T. Otani, Y. Nagao, M. Suzuki, and F. Kubota, "Stable 160 Gbit/s DPSK transmission using a simple PMD compensator on the field photonic network test bed of JGN II", Proc. OECC 2004, PD-1-3.

43. F. Buchali, W. Baumert, M. Schmidt, and H. Buelow, "Dynamic distortion compensation in a 160 Gb/s RZ OTDM system: adaptive 2 stage PMD compensation", Optical Fiber Communication Conf., pp. 589–590 (2003)

44. S. Kieckbusch, S. Ferber, H. Rosenfeldt, R. Ludwig, A. Ehrhardt, E. Brinkmeyer, and H.G. Weber, "Automactic PMD compensator in a single-channel 160 Gb/s transmission over deployed fiber using RZ-DPSK modulation format" J. Lightwave Technol. **23** (1), 165–171 (2005).

45. M. Schmidt, M. Witte, F. Buchali, E. Lach, E. Le Rouzic, S. Salaun, S. Vorbeck, and R.Leppla, "8×170 Gbit/s DWDM Field Transmission Experiment over 430 km SSMF Using Adaptive PMD Compensation", ECOC 2004 Stockholm, PDP Th4.1.2.

46. M. Nakazawa, K. Suzuki, E. Yoshida, E. Yamada, T. Kitoh, and M. Kawachi, "160 Gbit/s soliton data transmission over 200 km", Electron. Lett. **31**, 565–566 (1995).

47. S. Kawanishi, H. Takara, T. Morioka, O. Kamatani, and M. Saruwatari, "200 Gbit/s, 100 km time-division-multiplexed optical transmission using supercontinuum pulses with prescaled PLL timing extraction and all-optical demultiplexing", Electron. Lett. **31**, 816–817 (1995).

48. S. Kawanishi, H. Takara, T. Morioka, O. Kamatani, K. Takiguchi, T. Kitoh, and M. Saruwatari, "Single channel 400 Gbit/s time-division-multiplexed transmission of 0.98 ps pulses over 40 km employing dispersion slope compensation", Electron. Lett. **32**, 916 (1996).

49. M. Nakazawa, E. Yoshida, T. Yamamoto, E. Yamada, and A. Sahara, "TDM single channel 640 Gbit/s transmission experiment over 60 km using 400 fs pulse train and walk-off free, dispersion flattened nonlinear optical loop mirror", Electron. Lett. **34**, 907–908 (1998).

50. T. Yamamoto, E. Yoshida, K.R. Tamura, K. Yonenaga, and M. Nakazawa, "640 Gbit/s optical TDM transmission over 92 km through a dispersion managed fiber consisting of single-mode fiber and reverse dispersion fibre", IEEE Photon. Technol. Lett. **12**, 353–355 (2000).

51. M. Nakazawa, T. Yamamoto, and K. R. Tamura, "1.28 Tbit/s–70 km OTDM transmission using third-and fourth-order simultaneous dispersion compensation with a phase modulator, Electron. Lett. **36**, 2027–2029 (2000).

52. S. Kawanishi, H. Takara, K. Uchiyama, I. Shake, O. Kamatani, and H. Takahashi, "1.4 Tbit/s (200 Gbit/s × 7 ch) 50 km optical transmission experiment", Electron. Lett. **33**, 1716–1717 (1997).

53. S. Kawanishi, H. Takara, K. Uchiyama, I. Shake, and K. Mori, "3 Tbit/s (160 Gbit/s × 19 channel) optical TDM and WDM transmission experiment", Electron. Lett. **35** (10), 826–827 (1999).

54. R. Ludwig, U. Feiste, S. Diez, C. Schubert, C. Schmidt, H.J. Ehrke, and H.G. Weber, "Unrepeatered 160 Gbit/s RZ single-channel transmission over 160 km of standard fibre at 1.55 μm with hybrid MZI optical DEMUX", Electron. Lett. **36**, 1405–1406 (2000).

55. U. Feiste, R. Ludwig, C. Schubert, J. Berger, C. Schmidt, H.G. Weber, B. Schmauss, A. Munk, B. Buchold, D. Briggmann, F. Kueppers, and F. Rumpf, "160 Gbit/s transmission over 116 km field-installed fibre using 160 Gbit/s OTDM and 40 Gbit/s ETDM", Electron. Lett. **37**, 443–445 (2001).

56. T. Yamamoto,U. Feiste, J. Berger, C. Schubert, C. Schmidt, R. Ludwig, and H.G. Weber, "160Gbit/s demultiplexer with clock recovery using SOA-based interferometric switches and its application to 120 km fiber transmission", ECOC'01, Amsterdam, Tu.L.2.6.

57. A. Suzuki, X. Wang, T. Hasegawa, Y. Ogawa, S. Arahira, K. Tajima, and S. Nakamura, "8×160Gb/s (1.28Tb/s) DWDM/OTDM unrepeatered transmission over 140 km standard fiber by semiconductor-based devices", ECOC 2003, Rimini, paper Mo3.6.1.

58. J.P. Turkiewicz, E. Tangdiongga, G.-D. Khoe, H. de Waardt, W. Schairer, H. Rohde, G. Lehmann, E.S.R. Sikora, Y.R. Zhou, A. Lord, and D.B. Payne, "Field trial of 160 Gbit/s OTDM add/drop node in a link of 275 km deployed fiber", in Proc. Optical Fiber Commun. Conf. 2004, Los Angeles, CA, PDP1.

59. D.D. Marcenac, A.D. Ellis, and D.G. Moodie, "80 Gbit/s OTDM using electroabsorption modulators", Electron. Lett. **34** (1), 101–103 (1998).

60. A.D. Ellis, J.K. Lucek, D. Pitcher, D.G. Moodie, and D. Cotter, "Full 10×10 Gbit/s OTDM data generation and demultiplexing using electroabsorption modulators", Electron. Lett. **34** (18), 1766–1767 (1998).

61. B. Mikkelsen, G. Raybon, R.-J. Essiambre, K. Dreyer, Y. Su, L.E. Nelson, J.E. Johnson, G. Shtengel, A. Bond, D.G. Moodie, and A.D. Ellis, "160 Gbit/s single-channel transmission over 300 km nonzero-dispersion fiber with semiconductor based transmitter and demultiplexer", ECOC 1999, postdeadline paper 2-3, Nice (1999).

62. J. Yu, K. Kojima, N. Chand, M.C. Fischer, R. Espindola, and T.G.B. Mason, "160 Gb/s single-channel unrepeatured transmission over 200 km of non-zero dispersion shifted fiber", Proc. ECOC 2001 paper PD M.1.10 (2001).

63. J-L. Augé, M. Cavallari, M. Jones, P. Kean, D. Watley, and A. Hadjifotiou, "Single channel 160 Git/s OTDM propagation over 480 km of standard fiber using a 40 GHz semiconductor mode-locked laser pulse source", OFC 2002, paper TuA3, Anaheim (2002).

64. E. Lach, M. Schmidt, K. Schuh, B. Junginger, G. Veith, and P. Nouchi, "Advanced 160 Gb/s OTDM system based on wavelength transparent 4×40 Gb/s ETDM transmitters and receivers", OFC 2002 Anaheim, paper TuA2.

65. H. Murai, M. Kagawa, H. Tsuji, K. Fujii, Y. Hashimoto, and H. Yokoyama, "Single Channel 160 Gbit/s (40 Gbit/s × 4) 300 km Transmission Using EA Modulator based OTDM Module and 40 GHz External Cavity Mode-locked LD", ECOC 2002, paper 2.1.4, Copenhagen.

66. M. Schmidt, E. Lach, K. Schuh, M. Schilling, P. Sillard, and G. Veith, "Unrepeatered 320 Gbit/s (8×40 Gbit/s) OTDM transmission over 80 km TeraLight^{TM}-reverse TeraLight^{TM} fiber link", ECOC 2003, We.4.P.117, Rimini.

67. B. Mikkelsen, G. Raybon, B. Zhu, R.-J. Essiambre, P.G. Bernasconi, K. Dreyer, L.W. Stulz, and S.N. Knudsen, "High spectral efficiency (0.53 bit/s/Hz) WDM transmission of 160 Gb/s per wavelength over 400 km of fiber", OFC 2001, paper ThF2-1, Anaheim.

68. K. Schuh, M. Schmidt, E. Lach, B. Junginger, A. Klekamp, G. Veith, and P. Sillard, "4×160 Gbit/s DWDM / OTDM transmission over 3×80 km TeraLight^{TM}-Reverse TeraLight^{TM}-fibre", ECOC 2002, paper 2.1.2, Copenhagen (2002).

69. M. Schmidt, K. Schuh, E. Lach, M. Schilling, and G. Veith, "8×160 Gbit/s (1.28 Tbit/s DWDM transmission with 0.53 bit/s/Hz spectral efficiency using single EA-modulator based RZ pulse source and demux", ECOC 2003, paper Mo3.6.5, Rimini.

70. E. Lach, K. Schuh, M. Schmidt, B. Junginger, G. Charlet, P. Pecci, and G. Veith, "7×170 Gbit/s (160 Gbit/s + FEC overhead) DWDM transmission with 0.53 bit/s/Hz spectral efficiency over long haul distance of Standard SMF", Proc. ECOC 2003 paper PD Th4.3.5.

71. M. Daikoku, T. Otani, and M. Suzuki, "160 Gb/s Four WDM Quasi-linear transmission over 225 km NZ-DSF with 75 km spacing", IEEE Photon. Technol. Lett. **15** (8), 1165–1167 (2003).

72. S. Randel, B. Konrad, A. Hodzic, and K. Petermann, "Influence of bitwise phase changes on the performance of 160 Gbit/s transmission systems", ECOC 2002 Copenhagen Proc., Vol.3, paper P3.31 (2002).

73. M. Kagawa, H. Murai, H. Tsuji, and K. Fujii, "Performance comparison of bitwise phase-controlled 160 Gbit/s signal transmission using an OTDM multiplexer with phase-correlation monitor", in Proc. ECOC 2004, paper We 4.P.109 (2004).

74. Y. Su, L.Moller, C. Xie, R. Ryf, X. Liu, X. Wei, and S. Cabot, "Ultra high-speed data signals with alternating and pairwise alternating optical phases", J. Lightwave Technol. **23** (1), 26–31 (2005).

75. A. Beling, H.-G. Bach, D. Schmidt, G.G. Mekonnen, R. Ludwig, S. Ferber, C. Schubert, C. Boerner, B. Schmauss, J. Berger, C. Schmidt, U. Troppenz, and H.G. Weber, "Monolithically integrated balanced photodetector and its application in OTDM 160 Gbit/s DPSK transmission", Electron. Lett. **39**, 1204–1205 (2003).

76. S. Ferber, R. Ludwig, C. Boerner, A.Wietfeld, B. Schmauss, J. Berger, C. Schubert, G. Unterboersch, and H.G. Weber, "Comparison of DPSK and OOK modulation format in 160 Gbit/s transmission system", Electron. Lett. **39** (20), 1458–1459 (2003).

77. T. Miyazaki, M. Daikoku, I. Morita, T. Otani, Y. Nagao, M. Suzuki, and F. Kubota, "Stable 160 Gbit/s DPSK transmission using a simple PMD compensator on the field photonic network test bed of JGN II", Proc. OECC 2004, PD-1-3.

78. S. Ferber, R. Ludwig, C. Boerner, C. Schubert, C. Schmidt-Langhorst, M. Kroh, V. Marembert, and H.G. Weber, "160 Gbit/s DPSK transmission over 320 km fibre link with high long-term stability" Electron. Lett. **41**, 200–202 (2005).

79. F. Ferber, C. Schmidt-Langhorst, R. Ludwig, C. Boerner, C. Schubert, V. Marembert, M. Kroh, and H.G. Weber, "160 Gbit/s OTDM long-haul transmission with long-term stability using RZ-DPSK modulation format" IEICE Trans. Commun. **E88-B** (5), 1947–1954 (2005).

80. V. Marembert, C. Schubert, S. Ferber, K. Schulze, C. Schmidt-Langhorst, C. Boerner, M. Kroh, R. Ludwig, S. Watanabe, F. Futami, R. Okabe, and H.G. Weber, "Single-channel 640 Gbit/s DPSK Transmission over a 160 km Fibre Link", Proc. Europ. Conf. on Opt. Comm. (ECOC'04), Stockholm, Sweden, 2004. Post-deadline paper Th4.4.2.

81. A.H. Gnauck and P.J. Winzer, "Optical phase-shift-keyed transmission", J. Lightwave Technol. **23** (1), 115–130 (2005).

82. A.Fauzi Abas Ismail, D. Sandel, A. Hidayat, B. Milivojevic, S. Bhandare, H. Zhang, and R. Noe, "2.56 Tbit/s,1.6 bit/s/Hz, 40 Gbaud RZ-DQPSK polarization division multiplex transmission over 273 km of fiber", OptoElectronic and Communication Conference, OECC 2004, Yokohama, Japan, PD-paper PD1-4 (2004).

83. B. Milivojevic, A.F. Abas, A. Hidayat, S. Bhandare, D. Sandel, R. Noé, M. Guy, and M. Lapointe, "1.6-bit/s/Hz, 160-Gbit/s, 230-km RZ-DQPSK Polarization Multiplex Transmission with Tunable Dispersion Compensation", IEEE Photon. Technol. Lett. **17** (2), 495 (2005).

84. S. Ferber, C. Schubert, R. Ludwig, C. Boerner, C. Schmidt-Langhorst, and H.G. Weber, "640 Gbit/s DQPSK Single-channel Transmission over 480 km Fibre Link", Electron. Lett. **41**, (22), 1234–1235 (2005).

85. H.G. Weber, S. Ferber, M. Kroh, C. Schmidt-Langhorst, R. Ludwig, V. Marembert, C. Boerner, F. Futami, S. Watanabe, C. Schubert, "Single Channel 1.28 Tbit/s and 2.56 Tbit/s DQPSK Transmission", Electron. Lett. **42**, 178–179 (2006).

DOI: 10.1007/s10297-004-0022-0
Originally published in J. Opt. Fiber. Commun. Rep. 2, 1–31 (2005)

Semiconductor mode-locked lasers as pulse sources for high bit rate data transmission

Leaf A. Jiang[1], Erich P. Ippen[1], and Hiroyuki Yokoyama[2]

[1] Research Laboratories of Electronics
Massachusetts Institute of Technology
Cambridge, MA 02139, USA

[2] New Industry Creation Hatchery Center (NICHe)
Tohoku University
10 Aramaki-Aza-Aoba, Aoba-ku, Sendai, Miyagi 980-8579, Japan

Abstract. Semiconductor mode-locked lasers are evaluated as pulse sources for high bit rate data transmission. This chapter describes the requirements of OTDM sources for high bit rate data transmission, compares various OTDM source technologies, describes three semiconductor mode-locked laser cavity designs, explains the impact of timing jitter and amplitude noise on OTDM performance, illustrates how to characterize noise of OTDM sources using rf and optical techniques, shows how to interpret the noise measurements, and finally discusses semiconductor mode-locked laser cavity optimizations that can achieve low noise performance.

A critical part of the design of a communication system is the choice of the transmitter or source laser. High bit rate optical time-division multiplexed (OTDM) systems in particular demand reliable short pulse generation at high repetition rates and turn-key operation. Semiconductor mode-locked lasers are becoming increasingly attractive and viable for such applications.

Semiconductor mode-locked lasers can be compact sources of picosecond, high-repetition rate pulses of light at the popular telecommunication wavelength of 1.5 μm [1, 2]. Recent advances in semiconductor processing and cavity design have led to the advent of ultra-stable [3] and ultralow-noise [4, 5] performance. With proper temperature control of the semiconductor device and a clean electric supply for the bias and injection current, the diode can remain mode-locked for days. Single-channel, single-polarization transmission rates up to 160 Gb/s [6] have been successfully demonstrated using mode-locked semiconductor lasers, and detailed characterization of their noise

properties [4] indicate that they may be useful sources for transmission rates beyond 1 Tb/s.

The next two sections will discuss several mode-locked semiconductor laser designs and how the performance of these lasers impacts the bit error rates of OTDM systems. The latter sections will show how to measure the noise of these lasers, describe the physical origins of the measured noise spectra, and discuss the ultimate limits of their timing jitter performance.

1. Requirements for OTDM Sources

The requirements for an OTDM pulse source can be listed as follows

1. **Short pulses.** Single channel rates of 160 Gbit/s (6.25 ps/bit-slot) and 1.28 Tbit/s (0.78 ps/bit-slot) require pulses that are a fraction of the repetition period.
2. **High repetition rate.** The source repetition rate should ideally match the rate at which opto-electronic modulators can impress data onto a pulse train. Currently, this rate is typically 10 or 40 GHz. These 10 or 40 Gbit/s data streams can then be multiplexed up to higher repetition rates using passive delay lines. For example, a 10 Gbit/s data pulse train was multiplexed up to a 640 Gbit/s signal using a planar lightwave circuit multiplexer [7]. The highest aggregate repetition rate is limited by the pulse width.
3. **Low pedestal, high extinction ratio.** A low extinction ratio between intensity of the peak of a data pulse and intensity in the wings causes channel crosstalk and interferometric noise due to the fluctuating phase difference of neighboring pulses [8]. For example, a 40-dB extinction ratio is required to interleave four 10 Gbit/s OTDM channels with negligible penalty due to interference [9]. This extinction ratio is easily achieved with Erbium-doped fiber lasers ($>$ 40 dB), but difficult to achieve with electro-absorption modulators and $LiNbO_3$ modulators (15-25 dB) [10].
4. **Low timing jitter.** Experiments and theory [8] have shown that the timing jitter should be less than 1/12 of the switching window width of the demultiplexer to achieve a bit error rate (BER) of less than 10^{-9} for a signal pulse whose width is equal to 1/5 the time slot width. For example, a 100-Gbit/s OTDM system with a demultiplexer that has a 5-ps switching window should have a signal source with better than 0.42 ps rms timing jitter [11].
5. **Low amplitude noise.** The amplitude noise of a pulse source is directly related to the BER of an OTDM system. Often the amplitude noise of a cw laser source is characterized by its relative intensity noise (RIN), which is the ratio of the variance to the squared mean of the output intensity.
6. **Locked to standard clock rate.** The repetition rate of the pulse source must be able to lock to a standard repetition rate, e.g., the synchronous digital hierarchy (SDH) frequencies of 9.953, 19.906, and 39.813 GHz [12]. For mode-locked laser sources, the laser cavity must either be actively or hybridly mode-locked, or passively mode-locked with feedback to stabilize the repetition rate to a known rf reference.

7. **Highly reliable and stable.** The ability to have turn-key operation with reliable performance, minimal tweaking, and long-term operation is desirable. Long-term stability has been demonstrated with both semiconductor [1, 3] and fiber lasers [13, 14, 15].

Erbium-doped mode-locked fiber lasers, compressor sources, gain-switched laser diodes, and mode-locked semiconductor lasers have each been shown to satisfy most, if not all, of the above requirements. The next section will compare the performance of these sources for OTDM applications.

2. Comparison of OTDM Sources

2.1. Mode-locked Erbium-Doped Fiber Laser (ML-EDFL)

ML-EDFLs are typically ring cavities that consist of the erbium-doped fiber, an electro-optic phase or amplitude modulator, isolators for unidirectional operation, and additional fiber for nonlinear/pulse-shaping effects. The erbium-doped fiber can be pumped at 980 or 1480 nm and typically provides gain from 1530-1610 nm [16]. Since these wavelengths correspond to the low attenuation wavelength region in silica-core fiber, erbium-doped fibers have been used extensively in optical transmission systems for amplification and laser sources.

ML-EDFLs are capable of generating picosecond pulses at multi-gigahertz repetition rates. Examples include 1.6 ps pulse generation at 40 GHz [17], 0.7-1.3 ps pulses at 10 GHz in the 1536-1569 nm wavelength region [18], 1.2-1.9 ps pulses at 40 GHz tunable over 40 nm [19], 1.3 ps pulses at 10 GHz [20], and 0.85 ps pulses at 40 GHz [21]. The reported pulse widths are transform-limited or near-transform-limited for hyperbolic secant pulses. Output average powers of ML-EDFL are typically on the order of 10 mW.

The advantages of the ML-EDFLs are that they have good pulse quality (typically transform-limited hyperbolic secant pulses), high extinction-ratio, low noise, and are a mature technology [13, 14, 15]. On the other hand, the ML-EDFLs are relatively large ($18 \times 48 \times 38$ cm are typical dimensions), are sensitive to environmental changes, require feedback circuits to stabilize the long fiber cavity length, and may suffer from pulse drop-outs.

2.2. Compressor Sources

A compressor source typically starts with a long pulse (tens of picoseconds) that is generated by a gain-switching a laser diode or modulating the output of a cw laser source. Compression of these long pulses through adiabatic soliton compression can result in sub-picosecond pulses [22]. Compressor sources have drawn much attention due to the simplicity of operation and availability of commercial components.

Adiabatic pulse compression by propagating amplified pulses through dispersion decreasing fiber (DDF) has been used to obtain short pulses [22]. The decreasing dispersion should be gradual on the timescale of the soliton period, which means that the required length of fiber grows quadratically with initial pulse width [23]. For a sinusoidal modulation at 10 GHz, the required DDF length to generate picosecond pulse

trains is close to thousands of kilometers [24]. Using a shorter length of DDF results in significant pedestals which need to be removed using a nonlinear amplifying loop mirror (NALM); but this reduces the required DDF length from hundreds of kilometers to less than 30 km [24]. The quadratic dependence of DDF length on the initial pulse width means that it is desirable to start with a short pulse, so that the length of the DDF length can be a reasonable length (less than several tens of kilometers). When an EAM was used to directly generate 6 ps pulses, only 2 km and 1.6 km of DDF were needed to obtain 1.2 ps (2.5 GHz, < -25 dB pedestal) and 0.19 ps (10 GHz, -23 dB pedestal) pulses [25, 26]. It has been difficult to date to obtain DDF with a consistently uniform dispersion profile. To overcome this limitation, comb-like dispersion profiled fiber (CDPF) has also been used [27]. CDPF consists of fusion-spliced sections of commercially available high and low dispersion fiber. Modest compression factors of 1:5 or 1:9 can be obtained since the maximum practical number of segments that can be included in a CDPF is $\approx$ 30 [28]. A new type of pulse compression using Raman gain in 6.75 km of standard Corning SMF-28 fiber has recently been shown to yield 1.3 ps pulses at 10 GHz that were nearly transform limited (TBWP = 0.32) [23]. This technique yielded an excellent pedestal of -27 dB without the use of a NOLM or DDF.

The advantages of compressor sources is that they can require little tweaking, yield high output powers, yield transform-limited pulses, can produce sub-picosecond pulses, and are readily constructible from standard telecom equipment. The disadvantages are that they require several large optical components, require several kilometers of single-mode fiber which is temperature and polarization sensitive, and may require hard-to-obtain specialty DDF. The amplitude and timing noise of these sources is not well characterized, and they can have large pedestals (although that can be fixed with a NOLM or clever design). Furthermore, fluctuations of the effective length of the kilometer-long pulse compressor fiber necessitates the use of active stabilization of the fiber length to allow effective multiplexing of several compressor sources into one high data-rate OTDM source.

2.3. Gain-Switched Laser Diode

Short pulses can be obtained from laser diodes by biasing the gain region below threshold and using a pulse or sinusoidal injection current [11]. The achievable modulation frequency in a gain-switched laser diode is limited by its relaxation frequency, which is usually less than 30 GHz [11]. Short, chirped pulses of 20-30 ps duration can be obtained and can be compressed to 2-6 ps by passing them through a normal dispersion medium [11]. In one experiment, 20 fs pulses were generated using a four-stage soliton compression technique [29], but there were significant pedestals containing half the pulse energy that extended for approximately 100 fs.

Pulses with a pulse width of 0.42 ps at a 100-MHz PRF with 1.3 ps of pulse-to-pulse timing jitter were obtained by using a gain-switched DFB-LD with CW light injection and nonlinear optical loop mirror [30]. The timing jitter was reduced from 7.1 to 1.3 ps with the CW light injection. Loss-switching instead of gain-switching of a two-section laser diode at 5 GHz with 30 ps pulses yielded an uncorrelated timing jitter of 0.25 ps. The better performance is presumably due to the better extinction ratio and sharper modulation curvature of loss-modulation. Similar timing jitter performance can be obtained by gain-switching and employing optical and electrical feedback [31].

At high modulation frequencies (> 10 GHz), the timing jitter of a gain-switched laser diode is almost the same as that of the RF oscillator used to drive the LD [11]. The timing jitter gets worse at lower modulation frequency (< 1 GHz) since the spontaneous emission noise can build up over a larger time. It was also found experimentally [32], that the timing jitter becomes worse as the DC bias is adjusted to obtain short pulse operation. The timing jitter of a DFB-LD driven at 5 GHz had uncorrelated jitter of 2 ps with a pulse width of 6 ps and a jitter of 0.5 ps with a pulse width of 10 ps [32]. The uncorrelated timing jitter from the driving synthesizer remained at a constant 0.2 ps. Uncorrelated timing jitter is the pulse-to-pulse timing jitter that arises from the random turn-on process from ASE buildup.

The advantages of gain-switched laser diodes are that they are turn-key ready, reliable, compact, and repetition-rate tunable. The disadvantages are that they require a bulky normally dispersive element such as dispersion compensating fiber to compress the pulses, pulse widths of gain-switched lasers are typically 20-30 ps, and they suffer from significant uncorrelated timing jitter, which is typically on the order of 1-2 ps. In addition, the shape, width, and frequency of every pulse is different and depends on the statistics of the spontaneous emission at the time the gain is increased, especially for very short pulses [33].

2.4. Mode-locked Semiconductor Laser

The first mode-locked semiconductor laser in AlGaAs was demonstrated by P. T. Ho in 1978 [34]. Since then, the pulse widths of mode-locked semiconductor lasers have dropped from 30 ps down to 1 ps [1, 3, 35].

Semiconductor mode-locked lasers can directly yield short pulses of durations ≈ 1 ps. They are widely wavelength tunable since the semiconductor gain medium can be designed to encompass a broad range of wavelengths. Their compact size allows fundamental modelocking, which results in stable operation and prevents pulse drop-outs that may occur in harmonically mode-locked lasers. Small packaging allows integration of a thermoelectric cooler and thermistor to regulate the temperature of the diode chip and to allow long, reliable operation.

The disadvantages are that the output is slightly chirped (TBWP < 0.45 are typical), the output power of current devices are on the order of 1 mW, and the limited ability to create perfect AR coatings yields small satellite pulses that are typically 20 dB smaller than the main pulse.

A comparison of these various OTDM pulse sources are tabulated in Table 1.

3. Semiconductor Mode-locked Laser Designs

Semiconductor mode-locked lasers can be classified into three categories: the type of cavity (monolithic or external), the type of modelocking (passive, active, or hybrid), and the order of modelocking (fundamental or harmonic). A monolithic cavity is one in which all laser elements are integrated on the chip: modulator, saturable absorber, gain section, and gratings. An external cavity is one in which the cavity is formed by the laser diode device plus a free space section and mirror or grating. External cavities are desirable for low-repetition rates (2-10 GHz) where the monolithic device

Table 1. A comparison of various OTDM pulse sources. SL = Semiconductor Laser. CS = Compressor Source. EL = Erbium-fiber Laser. EC = External Cavity. M = Monolithic. FM = Fundamentally Mode-locked. HM = Harmonically Mode-locked. NR = Not Reported. † = coupled into single-mode fiber. ‡ = obtained by integrating the first supermode. ♣ = 1545-1560 nm tunable for 1 ps pulse widths. ♡ = 90 fs free-run

Pulse Source Type	Output Power	Pulse Width	TBWP	Repetition Rate	Wavelength	Timing Jitter	RIN	Ref.
Semiconductor laser (EC-FM)	-6 to 6 dBm	> 1.5 ps	< 0.45	2-10 GHz	1520-1560 nm	86-500 fs	< 140 dB/Hz	[3, 4]
(EC-HM)	-6 to 6 dBm	> 1.5 ps	< 0.45	40 GHz	1530-1570 nm	86-500 fs	< 140 dB/Hz	[36]
Semiconductor laser (EC-FM)	-5 dBm	0.2-20 ps	???	1-20 GHz	1480-1580 nm	300-800 fs	NR	[1]
Semiconductor laser (M-FM)	0.5 mW	1.6 ps	0.52	80 GHz	1554 nm	230 fs	< -125 dB/Hz	[37]
	NR	2.4 ps	0.45	102 GHz	1554 nm	230 fs	< -125 dB/Hz	[37]
	2.9 dBm †	4 ps	0.5	20 GHz	1556 nm	200 fs	-129 dB/Hz @ 1.8 GHz	[38]
	NR	2 ps	1.2	16.3 GHz	1590 nm	NR	NR	[39]
Semiconductor laser (M-FM)	NR	4 ps	1.4	40 GHz	1.5 μm	NR	NR	[40]
Semiconductor laser (M-FM)	-8 dBm	0.95 ps	0.32	38.5 GHz	1.5 μm	NR	NR	CPM [41, 42]
Semiconductor laser (M-FM)	0.183 mW†	6.7 ps	0.38	10 GHz	1551 nm	0.3 ps	NR	Rep-rate tunable [12]
	NR	8.3 ps	0.32	20 GHz	1548.5 nm	0.18 ps	-140 dB/Hz	Rep-rate tunable [12]
	NR	NR	NR	40 GHz	NR	0.2 ps	NR	Rep-rate tunable [12]
Semiconductor laser (M-FM)	0.1 mW†	8 ps	0.30	4.9 GHz	1565.4 nm	NR	NR	[43]
	NR	20 ps	0.34	8.1 GHz	1550 nm	NR	NR	[44]
Semiconductor laser (M-FM)	0.5 mW	1.4 ps	NR	15 GHz	1.3 μm	NR	NR	[45]
Semiconductor laser (M-FM)	0.63 mW	2.2 ps	1.1	21 GHz	1.58 μm	NR	NR	[46]
Semiconductor laser (M-FM)	≥ 1 mW†	2-2.5 ps	0.37-0.5	37.5GHz$\pm$250MHz	1.5μm$\pm$2.5nm	300 fs(100Hz-80MHz)	NR	[?]
Compressor source	27 dBm	1.2 ps	0.32	10 GHz	1547-1558 nm	NR	NR	[23]
Compressor source	> 40 mW	190 fs	0.38	10 GHz	1566 nm	NR	1%	[47]
Compressor source	NR	130 fs	0.313	6.67-18 GHz	1550 nm	NR	NR	[48]
Compressor source	120 mW	560 fs	NR	10 GHz	1534-1560 nm	NR	NR	5% pedestals [49]
Erbium-fiber laser (HM=9960)	8.3 mW	1.3 ps	0.62	10 GHz	1564 nm	0.16 ps ‡	1.1% ‡	AM sigma laser [20]
Erbium-fiber laser (HM=200000)	NR	1.6 ps	Near TL	40 GHz	1556 nm	0.46 ps ‡	NR	AM [17]
Erbium-fiber laser (HM=6500)	3.4-5.2 mW	0.7-1.3 ps	0.31-0.33	10 GHz	1536-1569 nm	110 fs ‡	NR	AM [18]
(HM=24000)	14 dBm	1.2-1.9 ps	0.32-0.35	40 GHz	1530-1570 nm	< 0.1 ps ‡	NR	AM [19]
Erbium-fiber laser (HM=44444)	4 mW	0.85-1.1 ps	0.37-0.42	40 GHz	1540-1555 nm	NR	NR	Regen [21]
(HM=44444)	2-4 mW	0.9-1.3 ps	0.3	40 GHz	1530-1560 nm	< 0.1 ps ‡	NR	Regen [50]
(HM=11111)	NR	1 ps	TL	10 GHz	NR	120 fs PLL ‡♡	0.2% ‡	Regen [51]
(HM=11111)	1 mW	1-1.1 ps	0.35	10 GHz	1530-1555 nm	NR	NR	Regen [52]
Erbium-fiber laser (HM)	> 10 mW	1.6-10 ps	0.36	1-40 GHz	1530-1560 nm ♣	NR	NR	[13]
Erbium-fiber laser (HM)	> 20 mW	1.2-10 ps	NR	5-40 GHz	1530-1560 nm ♣	< 100 fs ‡	1.5% ‡	[14]
Erbium-glass laser (FM)	> 10 mW	3-5 ps	< 0.60	9.95328 GHz	1535 nm	< 100 fs	< 1.0 %	[15]

size becomes too large. Broad-band wavelength tuning is possible through the use of an optical filter or end-mirror grating, and precise tuning of the repetition rate by translating the end mirror or grating. A fundamentally mode-locked laser only has one pulse in the cavity at any instant of time. A harmonically mode-locked laser has several pulses in the cavity and the repetition rate of the pulses is at an integer multiple (> 1) of the fundamental cavity round-trip frequency. The preferable configuration for a mode-locked semiconductor laser is a monolithic cavity (for compact packaging) that is fundamentally (to prevent pulse drop-outs) and hybridly mode-locked (for short pulses).

This section is broken up into three parts which address external-cavity mode-locked lasers, monolithic mode-locked lasers and harmonically mode-locked lasers.

3.1. External-Cavity Mode-locked Laser

The basic design of an external-cavity mode-locked laser is shown in Fig. 1. The laser diode chip contains a saturable absorber section and a gain section (typically InGaAsP-based for operation in 1.3 or 1.5-μm wavelength regions). The external cavity contains a GRIN lens, an optical bandpass filter, and an end-mirror. The filter and mirror can be replaced by a grating for wavelength and repetition-rate tunability. Although bulk optics are used, these devices can be packaged into compact 33 x 21 x 10 mm boxes [3].

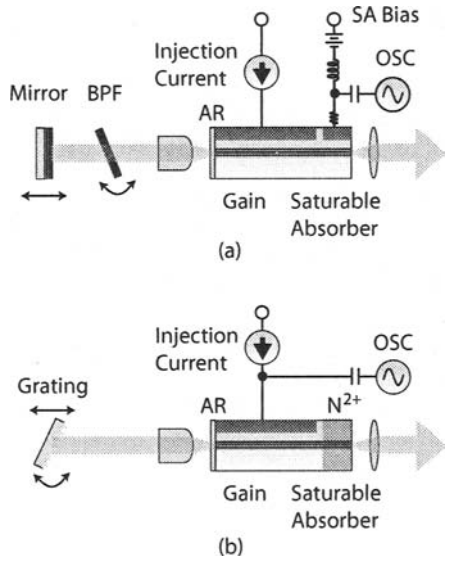

Fig. 1. Basic design of an external cavity mode-locked semiconductor laser with (a) optical bandpass filter [3] and (b) grating [35].

External-cavities allow broad wavelength tuning(120 nm) as well as repetition-rate tuning (1-14 GHz) [1, 35]. Fundamental modelocking is possible to 14 GHz, beyond which the cavity length becomes too small for bulk components. Higher modulation rates require either harmonic modelocking or monolithic devices.

Pulse widths down to 180 fs with external-cavity mode-locked lasers have been demonstrated [35], but repeatability of the saturable absorber properties and short pulse instabilities have limited practically obtainable pulse widths to > 1 ps.

The saturable absorber in the mode-locked semiconductor laser allows pulse widths shorter than the usual Siegman-Kuizenga limit [53, p. 1067]. One facet of the laser diode can be N^+-ion implanted to create a saturable absorber [35]. Alternatively, the saturable absorber can also be created by reverse biasing a short segment of the laser to create a waveguide saturable absorber [3, 46]. The second method can be manufactured more reliably but may yield absorbers with slower recovery times. The mode-locked laser yielding 180 fs pulses had an ion-implantation-type saturable absorber [35].

A schematic of a bi-section MLLD device is shown in Fig. 2. The device is a double-channel planar buried heterostructure laser diode with a separate confinement heterostructure with InGaAs/InGaAsP strained MQWs for the active layer [54]. The gain section is 500 μm long and the saturable absorber section is 40 μm long. Typical operating specifications for these mode-locked lasers is shown in Table 1, Ref. [3].

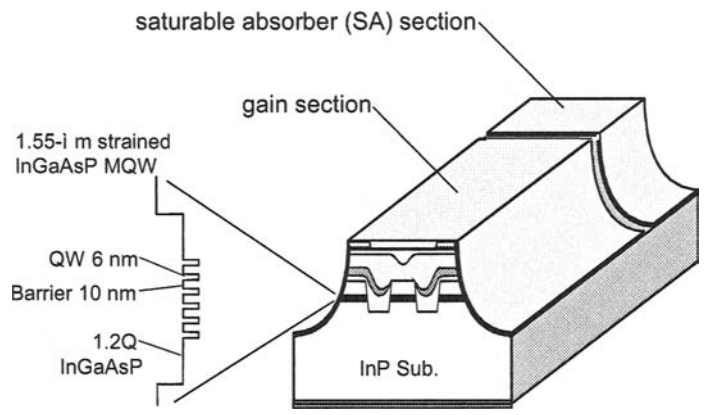

Fig. 2. The double-channel buried heterostructure MLLD device with a separate confinement heterostructure with InGaAs/InGaAsP strained MQWs for the active layer [3].

3.2. Monolithic Mode-locked Laser

Ideally, the OTDM pulse source should be a monolithic device that does not consist of external components [39, 41, 43, 44]. Such a source would be more compact, permit reduced cost in fabricating a number of devices, and not have the mechanical instabilities associated with bulk optical elements. Monolithic mode-locked lasers have multiple segments, often including a waveguide saturable absorber, gain section, electro-absorption modulator, and DBR section. Figure 3 shows an example of a repetition-rate tunable mode-locked laser diode.

The main challenge with monolithic devices is to achieve precise repetition-frequency control by cleaving a precise cavity length. To tune the cavity length of

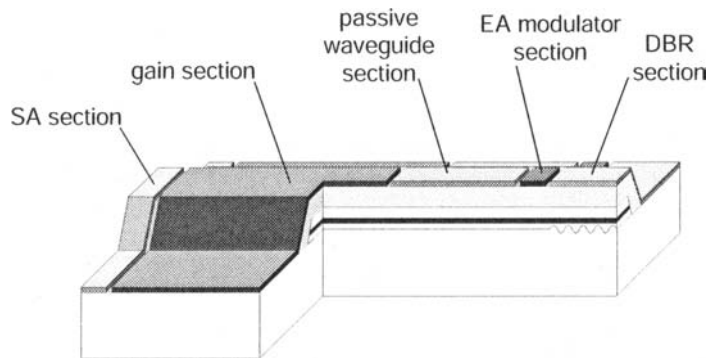

Fig. 3. Monolithic MLLD device structure [12].

a monolithic device to an exact frequency of 9.953, 19.906, or 39.813 GHz, an electrically tuned DBR section can be integrated into the device to fine-tune the effective cavity length [12, 55]. A typical fabrication error in cleaving a diode chip is 10 μm. Ogura et al. have shown that it is possible to compensate for this error with a small change in the absorption loss in the DBR section of about 20 cm^{-1} [12]. The detuning range of a monolithic mode-locked laser at 20 GHz repetition rate can be 0.22 GHz (corresponding to an error of 22 μm) due to the retiming function of the electroabsorption modulation gate [38, 56]. Over this detuning range, this particular laser emitted 4 ps pulses with a TBWP of 0.5. The downside of this technique is that the detuning is accompanied by a wavelength shift. To overcome this problem, multiple tuning elements consisting of electronic and thermal phase tuning sections were used [**?**]. Recently, a 2-2.5 ps pulse width, 220 fs (100 Hz to 10 MHz) timing jitter, 40 GHz monolithic mode-locked laser with a 500 MHz repetition-rate tuning range has been demonstrated [**?**].

Typical performances of monolithic mode-locked semiconductor devices is shown in Table 1. The pulse widths of mode-locked semiconductor lasers are still far from the inherent gain bandwidth limit of $\approx$ 50 fs [57], and there remains work to be done in designing fast saturable absorbers to achieve shorter pulses.

3.3. Harmonically Mode-locked Laser

For ultimate flexibility in the design of the cavity elements, semiconductor ring lasers have been used [5]. These lasers are typically several meters long since they incorporate bulk devices such as a semiconductor optical amplifier (SOA), Faraday isolator, polarization controllers, and electro-optic modulator (see Fig. 4). Harmonic modelocking allows pulse repetition rates of 10 GHz and beyond, similar to that in mode-locked Erbium-doped fiber ring lasers. Repetition rates as high as 20 GHz and pulse widths as short as 1.2 ps have been demonstrated [5].

One inherent problem of harmonically-mode-locked lasers is the occurrence of pulse drop-outs and supermode noise. However, the incorporation of a high finesse Fabry-Perot (F-P) etalon removes the supermode noise by distributing the pulse energy of one pulse to many other time slots [58, 59, 60]. Timing jitter as low as 165 fs from

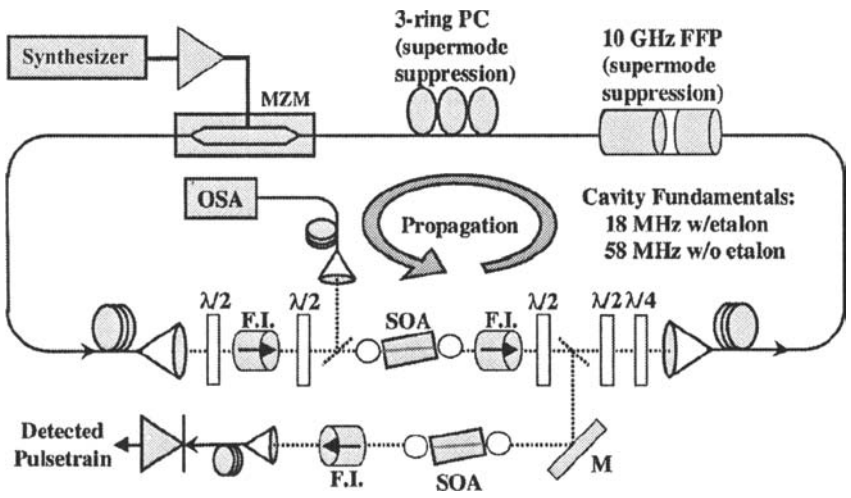

Fig. 4. Harmonically mode-locked semiconductor diode ring laser with intracavity Fabry-Perot etalon [58].

10 to 5 GHz of a 10-GHz semiconductor diode ring laser with a F-P etalon has been reported [58]. Higher finesse F-P etalons may enable even lower timing jitters on the order of tens of femtoseconds. If a mode-locked laser source has 500 fs of timing jitter, incorporating a F-P etalon with finesse F, the timing jitter improves according to that shown in Table 2. The main difficulty with the incorporation of the Fabry-Perot etalon is matching the cavity modes with the F-P modes, and the alignment becomes more difficult as the finesse increases.

Table 2. Timing jitter improvement with Fabry-Perot etalon. σ = rms timing jitter, N = harmonically modelocking order, $\mathcal{F}$ = finesse.

N	$\sigma \propto N^{-1/2}$	$\mathcal{F} \propto N$
1	500 fs	–
180	37 fs	180
10000	5 fs	10000

The benefit of a harmonically mode-locked laser is the flexibility of cavity design which allows for picosecond pulses at high repetition rates with low noise. The drawback of using harmonically mode-locked lasers is their large size and mechanical sensitivity.

4. Noise of Semiconductor Mode-locked Lasers

This section will cover the impact of timing jitter and amplitude noise on OTDM performance, review techniques to characterize and interpret noise measurements, and present a brief overview of low noise laser design.

4.1. Impact of Timing Jitter and Amplitude Noise on OTDM Performance

Amplitude noise and timing jitter degrades the performance of OTDM transmission systems. This subsection derives the values of timing jitter and RIN needed to achieve a given transmission rate.

4.1.1. Timing Jitter

Often the rms timing jitter is quoted as a single number without indication of the integration range of the timing jitter noise power spectral density. Unfortunately, the rms timing jitter integration range is not standardized, and reported values can cover ranges of 100 Hz to 1 MHz [61], 10 Hz to 5 GHz [4, 62], etc. This makes it difficult to directly compare the noise of different mode-locked laser sources. So what integration range is important for OTDM systems? Since it is timing jitter relative to the recovered clock, not relative to the universe, that is important for evaluation of the BER, one must carefully interpret how the quoted timing jitter (relative to the universe) relates to the jitter relative to the recovered clock.

The recovered clock is derived from a data pulse train with timing jitter. The best performance of a clock recovery circuit occurs when all the incoming data bits are ones. Typically the low-pass filter, of bandwidth B, after the optical, electro-optical [63] or microwave [64] phase comparator determines the number of pulses (assuming all ones) over which the recovered clock is defined. Therefore, the recovered clock follows slow timing drifts and errors arise from fast timing fluctuations that occur faster than $1/B$, where B is typically 10 or 100 Hz. Slow timing fluctuations are important, since neighboring channels should not drift into each others time slots, but this slow drift can be actively compensated with feedback and is generally not a fundamental limitation.

Experiments and theory [8] have shown that the timing jitter (integrated for frequency offsets greater than B) should be less than 1/12 of the switching window width of the demultiplexer to achieve a bit error rate (BER) of less than 10^{-9} for a signal pulse whose width is equal to 1/5 the time slot width. For example, at 640 Gbit/s, the time slot width is 1.56 ps. A signal pulse 1/5 this duration has a duration of 313 fs and a switching window of half the time-slot has a duration of 781 fs. This would imply that the timing jitter should be less than $1/12 \times 781$ fs $= 66$ fs! See Table 3 for the required timing jitter performance at different repetition-rates. Therefore, at high aggregate bandwidth, timing jitter is a critical factor in the performance of an OTDM system. One can partially overcome the stringent timing jitter requirements by transmitting the clock with the data. Transmission at 640 Gbit/s $\times 2$ (for polarization multiplexing) has been demonstrated using regeneratively mode-locked fiber lasers [7]. The fact that the clock was transmitted with the signal alleviated the problem of timing jitter, since the jitter between the transmitted clock and laser is very small. One

can use a noisy laser, as long as one also transmits the noisy clock as well. Clock recovery from a 160 Gbit/s data stream typically yields timing jitters of 300 fs [63] and 230 fs [64], which is too large for 640 Gbit/s transmission. Therefore, transmission rates at 640 Gbit/s are possible, but may require the broadcasting of a master clock (to the receiver and other transmitting lasers) due to timing jitter. It will in any case be a challenge to lock multiple transmitting lasers to a master clock (derivable from one of the regeneratively mode-locked fiber lasers) with a residual jitter of less than 66 fs. In the reported 640 Gbit/s $\times 2$ transmission experiment [7], the high-repetition-rate OTDM transmission was derived by transmitting a 10 Gbit/s pulse train through a PLC MUX, rather than multiplexing 64 independent mode-locked laser sources. Therefore, it is important to develop sources with low residual phase noise [4, 5, 65]. The lowest reported residual phase noise for gigahertz-repetition-rate semiconductor lasers is 50 fs (100 Hz to 100 MHz, 12 ps pulse width) [65], 86 fs (10 Hz to 4.5 GHz, 6.7 ps pulses) [4], and 94 fs (10 Hz to 5 GHz, 3.5 ps) [58]. Even though the gigahertz-repetition-rate mode-locked erbium-doped fiber laser literature reports timing jitters of $<$ 10 fs (100 Hz to 1 MHz, 1 ps pulse width) [61], 16 fs (100 Hz to 100 kHz, 3 ps) [66], 120 fs (100 Hz to 10 MHz, 1 ps) [51], the total timing jitter should be integrated out to half the repetition-rate of the laser (i.e. 10 Hz to 5 GHz) [58, 67], and hence the total timing jitter of these sources are not well characterized since these integration ranges do not include the supermode timing jitter. In section 4.4, the design path towards sub-66 fs timing jitter sources will be outlined to enable multi-terabit per second transmission rates.

Table 3. Bitrate versus required timing jitter performance for a BER $< 10^{-9}$.

Bit rate (GHz)	Time Slot (ps)	Switching Window (ps)	Pulse Width (ps)	Allowable Timing Jitter (ps)
1	1000	500	200	42
10	100	50	20	4.2
40	25	12.5	5	1.05
160	6.25	3.13	1.25	0.26
640	0.16	0.78	0.31	0.66
1280	0.08	0.04	0.16	0.03

4.1.2. Amplitude Noise

In addition to timing jitter, amplitude noise can also worsen the BER of OTDM transmission. The relative intensity noise (RIN) is defined as the variance over the squared mean of the output intensity. For a BER $< 10^{-9}$, the laser must have a RIN < -21.6 dB [68, p.222], which corresponds to an rms power fluctuation of 6.9×10^{-2} times the average power. Table 4 shows the maximum RIN per unit bandwidth (dB/Hz) for a BER $< 10^{-9}$ at several bit rates. The table shows that as the system bandwidth is increased, the laser RIN per unit bandwidth must decrease for the same BER.

Typical values for the amplitude noise are: 0.21% or -26.78 dB (10 Hz to 5 GHz) for harmonically mode-locked semiconductor ring lasers [5], 0.01% or -40 dB (10 MHz to 10 GHz) for monolithic hybridly mode-locked semiconductor lasers [12], -48 dB (10 Hz to 5 GHz)[3], 1.1% or -19.59 dB ($<$ 200 kHz) for mode-locked erbium fiber

Table 4. Digital transmission RIN requirements for a given bit rate and BER = 10^{-9}.

Bit rate (Gbit/s)	System Bandwidth (GHz)	RIN (dB/Hz)
1	0.5	-108.6
2	1	-111.6
10	5	-118.6
40	20	-124.6
160	80	-130.6
640	320	-136.7
1280	640	-139.7

sigma laser [20], 0.2% or -26.99 dB (10 Hz to 10 MHz) for PLL regeneratively mode-locked erbium-doped fiber laser [51].

4.2. Characterization of Timing Jitter

The measurement and interpretation of timing jitter for mode-locked semiconductor lasers is presented in this section. Special attention will be given to the correct interpretation of the harmonically mode-locked laser rf spectrum.

4.2.1. Overview of Measurement Techniques

Three techniques for the measurement of mode-locked laser noise will be presented: RF spectrum analyzer, residual phase noise measurement, optical cross-correlation.

RF Spectrum Analyzer The experimentally easiest, but most difficult to interpret, method for amplitude and timing noise characterization is detecting the optical pulse train with a photodiode and observing the resulting electronic current on an rf spectrum analyzer. To extract timing jitter and amplitude noise values from the rf spectrum, one must first assume a model for the correlation of the pulse-to-pulse timing jitter and amplitude noise for the laser. The model is different for

gain-switched lasers [32, 69, 70] – Each pulse builds up independently from ASE. Therefore, the timing jitter of each pulse is *uncorrelated* with all other pulses. There is also a smaller correlated noise component in gain-switched lasers that is attributed to the correlated noise of the driving microwave signal.

fundamentally mode-locked lasers [70, 71, 72] – The same pulse recirculates through the laser cavity, each time giving up a fraction of its photons. Therefore, the position and amplitude of neighboring pulses are highly *correlated.*

harmonically mode-locked lasers [67] – Neighboring pulses arise independently from ASE similar to a gain-switched laser (assuming that there are no coupling effects such as gain saturation effects and reflections), but the pulses are highly correlated every round-trip since it is the same pulse, similar to a fundamentally mode-locked laser. Hence the noise correlation function in a harmonically mode-locked laser is a mix between the gain-switched laser and fundamentally mode-locked laser correlation functions.

Fitting the model to the measured rf spectrum yields the timing jitter and amplitude noise.

The calculated rf spectrum of a gain-switched laser is shown in Fig. 5. The pulse shape is assumed be delta-function-like and hence the power at all harmonic frequencies is constant. In a real laser with finite pulse width, the harmonics are multiplied by an envelope function that decreases with increasing frequency. The rf spectrum of a delta-function-like pulse was plotted to reveal the frequency dependence of timing and amplitude noise. The timing jitter increases with the square of the frequency and the amplitude noise is constant with frequency.

The rf spectrum of a fundamentally mode-locked laser is similar to that of a gain-switched laser, except that the spectral envelope limitation is not usually observable since the pulse width of a fundamentally mode-locked laser is typically much shorter than the inverse bandwidth of the electronics, and the uncorrelated noise of a fundamentally mode-locked laser is typically well-below the noise floor of the rf spectrum analyzer. Figure5 shows that when the pulses are totally uncorrelated, the rf spectrum contains a background that increases as the square of the frequency. The correlated noise energy appears as skirts around the harmonics of the repetition rate. The noise skirts are proportional to the amplitude noise power spectral density plus the timing jitter power spectral density times the harmonic number squared. An important consequence is that the noise skirts at the higher harmonics of the repetition rate reveal the timing jitter of the laser.

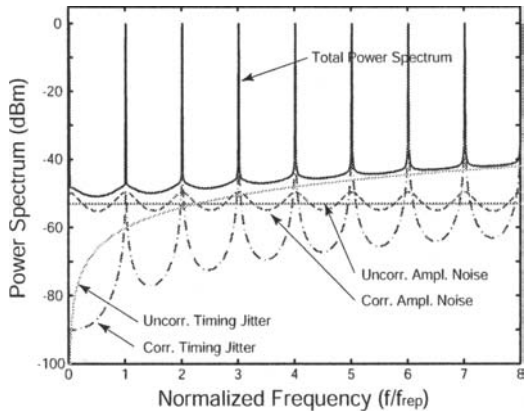

Fig. 5. The calculated rf spectrum of a gain-switched laser with correlated and uncorrelated noise. These calculations assumed that the pulse period $T_R = 100$ ps, the pulse width $FWHM \rightarrow 0$ ps, the rms correlated timing jitter $\sigma_{T,\mathrm{corr}} = 39.6$ fs, the rms correlated amplitude noise $\sigma_{A,\mathrm{corr}} = 1.77 \times 10^{-3}$, the uncorrelated timing jitter $\sigma_{T,\mathrm{uncorr}} = 100$ fs, the uncorrelated amplitude noise $\sigma_{A,\mathrm{uncorr}} = 2.24 \times 10^{-3}$. The correlated timing and amplitude noise spectra were assumed to be Lorentzian with a 3-dB bandwidth of 200 MHz and 4 GHz, respectively.

Harmonically mode-locked lasers have the addition of supermode noise that occurs at multiples of the cavity round-trip frequency. The power spectral density (psd) of the amplitude noise contributes equally to each supermode in the rf spectrum and the psd of the timing jitter contributes a noise skirt at each supermode whose magnitude increases as the square of the supermode number.

Rather than explain how to interpret the rf spectra in detail, we refer the reader to recent papers in the literature [67, 70]. The main point is that one must make assumptions about correlations of the pulse-to-pulse timing jitter and amplitude noise before the rf spectrum can be interpreted correctly and a valid rms timing jitter number can be obtained.

When using an rf spectrum analyzer to measure the noise of the laser, the measured result for the noise spectral density underestimates the noise by about 2 dB due to the effect of envelope detection, log averaging, and shape of the resolution filter of the rf spectrum analyzer [73].

Even though this method seems to be simple, actually measuring the power spectral density over many harmonics is not trivial. One must measure over several tens of gigahertz for a multiple number of spans and resolution bandwidths to capture the uncorrelated and correlated jitter. In addition, the frequency response of the detector plus spectrum analyzer from 0 to 50 GHz is not flat and must be calibrated. Figure 6 shows the power spectrum around the first harmonic of a fundamentally mode-locked external-cavity semiconductor laser [74]. The timing jitter noise can be upper-bounded by assuming that all the noise around the first harmonic is due to correlated timing jitter (we assume that the amplitude noise fluctuations are small) and the tails fit well to a Lorentzian shape.

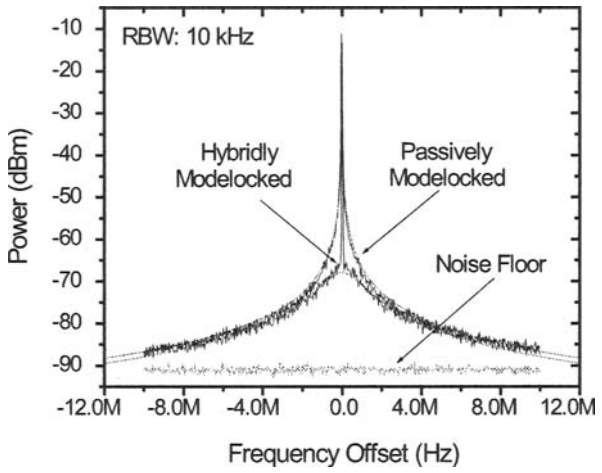

Fig. 6. RF measurements and Lorentzian fits. The span is 10 MHz [74].

Residual Phase Noise Measurement A residual phase noise measurement yields the timing jitter of the pulses relative to the driving microwave oscillator and is a good indication of the inherent quantum and technical noise of the mode-locked laser. The residual phase noise measurement method is illustrated in Fig. 7. A microwave oscillator drives a laser whose pulses are detected with a photodiode. The photodiode signal is then mixed with the original microwave oscillator signal. If the path length between the RF and IF ports of the mixer to the microwave oscillator are equal, then

the noise from the microwave source cancels. The mixer is operated as a phase detector by tuning the delay in one arm until the sinusoidal inputs to the IF and RF ports are in quadrature. The resulting phase noise can be measured with a rf spectrum or vector signal analyzer.

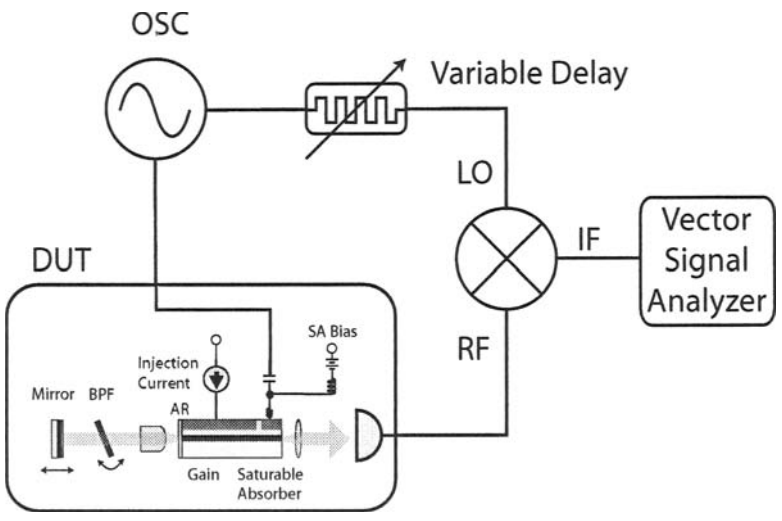

Fig. 7. The residual phase noise measurement of a optical pulse source.

The noise floor of the residual phase noise measurement is obtained by replacing the pulse source with an equivalent microwave loss. This loss was 51 dB in the case of an external-cavity hybridly-mode-locked semiconductor laser [4].

It is difficult to do residual phase noise measurements on a pulse train after fiber compression since it is difficult to match the length of the two arms to the mixer. In one arm there are several kilometers of single-mode fiber. Installing several kilometers of microwave cable in the other arm is impractical due to the large loss (typically 1 dB/m for SMA coaxial cables).

Until the advent of the ultralow-phase noise microwave sapphire-loaded crystal oscillator (SCLO) in 1996 (Poseidon Scientific Instruments), the noise of mode-locked lasers have been limited by the driving microwave source [65, 61]. At 10 GHz, the integrated timing jitter of the SCLO is $\approx$ 6 fs from 10 Hz to 5 GHz. This means that it is now possible to obtain mode-locked lasers with absolute timing jitters that are limited by their quantum noise [4].

Some residual phase noise measurements of mode-locked semiconductor lasers and the interpretation of the plots will be shown in section 4.2.2. The measurement of the noise of harmonically mode-locked lasers is especially difficult and will be discussed later.

Optical Cross-Correlation Optical cross-correlation techniques have been used extensively for characterizing the timing jitter between two lasers [75], the timing jitter of a gain-switched diode [30], and for mode-locked lasers [74]. The optical cross-correlation measurement is useful for measuring the timing jitter at high frequency

offsets (which is the same as the "uncorrelated jitter") and for directly measuring the timing jitter between pulses separated by time T. Several optical cross-correlation measurements with different values of T allows one to reconstruct the timing-jitter correlation function. Correlations between pulses that are separated by tens of thousands of pulse periods is possible at high repetition rates (10 or 40 GHz) using less than a kilometer of single-mode fiber as an optical delay line [74].

An optical cross-correlator is shown in Fig. 8. The input optical pulse train is split into two arms. Propagation in one arm is delayed relative to the other arm with a spool of fiber. The pulses from both arms are then recombined through a nonlinear crystal and the SHG is observed on a photomultiplier tube. The results of cross-correlation measurements made with a 1000-m delay are shown in Fig. 9. The three traces show the autocorrelation, cross-correlation, and autocorrelation preceded by the same 1000-m fiber spool. The broadening of the cross-correlation over the autocorrelation yields the timing jitter. The autocorrelation preceded by the same 1000-m fiber spool allows one to remove the broadening effects in the cross-correlation due to the dispersion of the fiber. The recovered rms timing jitter fluctuations as a function of fiber delay lengths from 20 to 500 m are plotted in Fig. 10 for both passively and hybridly mode-locked lasers. These two curves show that the timing jitter of the hybridly mode-locked laser is bounded due to the restoring force of the active modulator whereas the timing jitter of the passively mode-locked laser continues to increase as a function of delay, which is the theoretically expected result. Figure 10 shows a maximum timing jitter of approximately 700 fs, which also agrees with the integration of the rf spectrum measurement shown in Fig. 6. For higher modelocker modulation depths, the hybridly mode-locked laser can be as low as 159 fs (10 Hz to 10 MHz, see Fig. 11) with 2 ps pulses or 45 fs (10 Hz to 10 MHz, see Fig. 12) with 7 ps pulses [76].

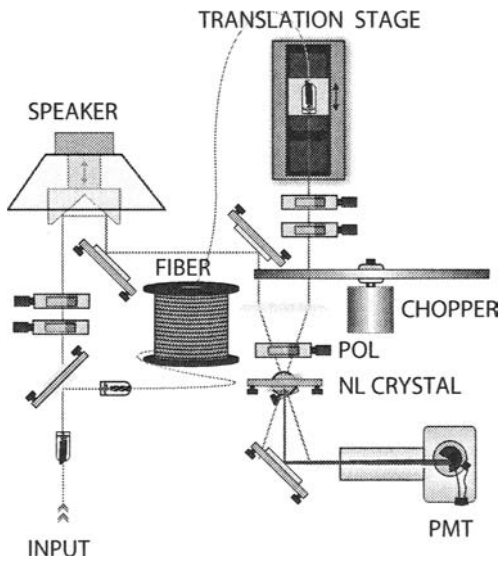

Fig. 8. An optical cross-correlator that measures the background-free SHG signal from a nonlinear crystal [74].

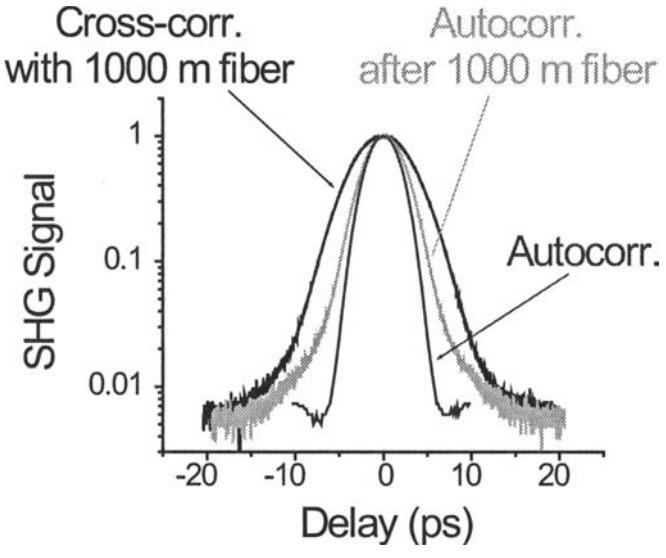

Fig. 9. Cross-correlation measurements.

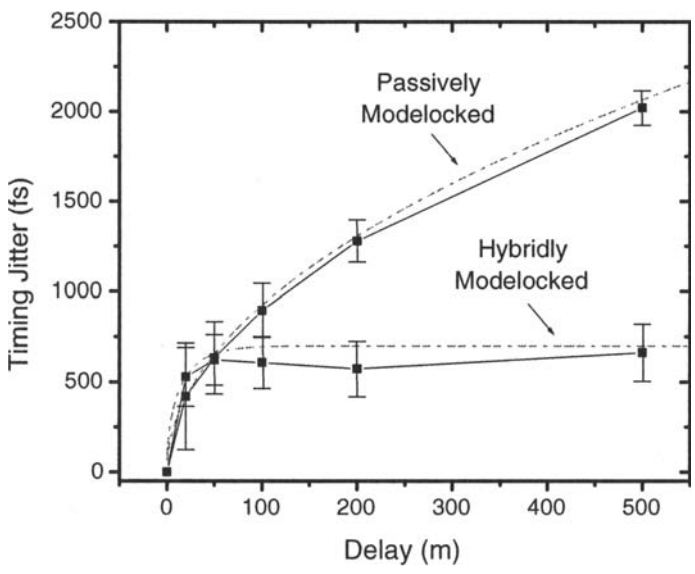

Fig. 10. Cross-correlation measurements of the timing jitter as a function of delay. The dashed lines indicate the theoretically predicted dependence [74].

Optical cross-correlations have also revealed the different timing jitter correlation functions of harmonically mode-locked lasers. In these lasers, the timing jitter is

highly correlated when T equals a multiple of the cavity round-trip time, but is highly uncorrelated otherwise.

4.2.2. Application of Measurement Techniques

The last subsection outlined three noise measurement techniques to determine the timing jitter of OTDM pulse sources. The interpretation of these measurements can be complicated, and in this subsection several important cases will be discussed.

Fundamentally and Actively Mode-locked Laser The pulse position perturbation in an actively mode-locked laser is analogous to that of a mass on a spring with damping but subject to white noise perturbations [77]. For dispersionless and AM modulated mode-locked lasers, the timing restoration of the pulses is critically damped. This means that once the pulse is perturbed from its equilibrium position, it moves back to its equilibrium position exponentially in time [78]. The power spectral density of a noise process with exponential retiming has a Lorentzian functional form.

The residual phase noise plots for a 2-ps-pulsewidth, 10-GHz, hybridly mode-locked external-cavity laser diode is shown in Fig. 11 [76]. The residual phase noise fits well to the theoretically expected Lorentzian shape plotted with a dashed line. Integrating from 10 Hz to 10 MHz yields rms timing jitters of 159 fs and 500 fs for an rf modulation strength of 24 and 15 dBm, respectively. The residual phase noise of an ultralow noise mode-locked semiconductor laser is shown in Fig. 12, which shows the noise spectral energy from 10 Hz to 4.5 GHz. The integrated values over each decade are shown in Fig. 13 and indicate that most of the integrated timing jitter arises around the spectral roll-off from 10 to 100 MHz. The integrated timing jitter from 10 Hz to 4.5 GHz is only 86 fs. At low offsets, flicker noise of the driving current source appears in the noise spectrum, but the effect on the integrated timing jitter is very small (< 8 fs).

Near-Lorentzian single-sideband phase noise has also been observed in other fundamentally and actively mode-locked external-cavity mode-locked laser diodes [1, 62]. For lasers that have dispersion in the cavity, active phase modulation, and other technical noise [37, 77], the phase noise spectra can be more complicated than a simple Lorentzian function.

Harmonically and Actively Mode-locked Laser The calculated rf spectrum of a harmonically mode-locked laser is shown in Fig. 14, and the calculated residual phase noise is shown in Fig. 15. The residual phase noise plot exhibits Lorentzian-shaped noise spectra that repeat at multiples of the cavity round-trip frequency. The high-frequency fluctuations are due to pulse-to-pulse fluctuations. Here it is assumed that each of the N pulses inside the laser cavity is uncorrelated with respect to all others[3] but is correlated with itself after an integer number of round-trips. Integrating the residual phase noise spectrum from 10 Hz to 5 GHz (half the repetition-rate) yields the timing jitter. Note that this measurement is difficult for two reasons:

1. Each Lorentzian spectrum should be measured over several decades 10-100 Hz, 100-1 kHz, ... 1-10 MHz, etc. If we measure 7 decades of offset, then $7N$ measurements are needed. For EDFLs, N is typically on the order of 10000, which

[3] This is a good approximation in EDFLs where the gain-lifetime is long, but may be less appropriate for semiconductor lasers where the gain strongly correlates neighboring pulses.

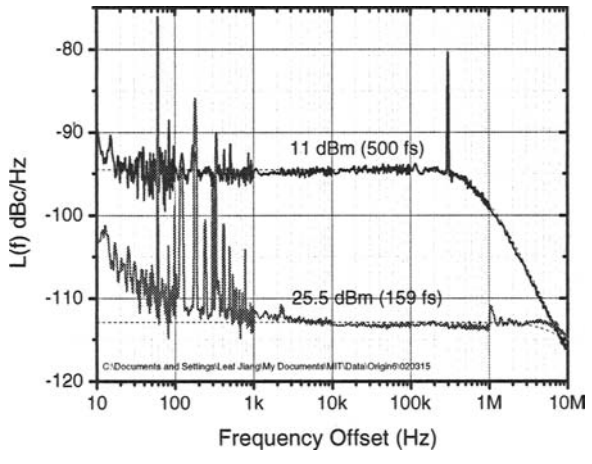

Fig. 11. Temperature-controlled external cavity mode-locked semiconductor laser with 5-nm filter for two different modulation depths.

means that to correctly measure the noise, one must run 70000 measurements! If we assume that neighboring pulses are uncorrelated, then all the Lorentzian spectra have the same height and only 7 measurements are needed.

2. The first supermode is most likely contaminated by the noise of the RF oscillator [79]. Assuming that a $N = 10000$ harmonically mode-locked laser has < 500 fs of jitter at a 10 GHz repetition rate (we know that this must be true from sampling scope measurements), then each Lorentzian supermode phase noise spectrum has only $\sqrt{500^2/N} = 5$ fs of timing jitter (assuming the pulses in the cavity are uncorrelated with respect to each other). If the FWHM of each Lorentzian is 50 kHz, then the phase noise is less -116 dBc/Hz from 10 Hz to 5 GHz! For the Agilent 83732B, the phase noise is only that good at offsets above 100 kHz. This means that the first supermode is mainly rf oscillator noise, as has been measured by several groups [61, 66].

To summarize, the procedure to measure the phase noise of a harmonically mode-locked laser is

1. measured one of the supermodes, but not the first few which are contaminated by the rf oscillator noise, over several decades
2. keeping the resolution bandwidth fixed, measure the relative heights of each supermode, assume that they all have the same shape as the one measured in the first step
3. integrate the supermodes from 10 Hz to half the repetition rate.

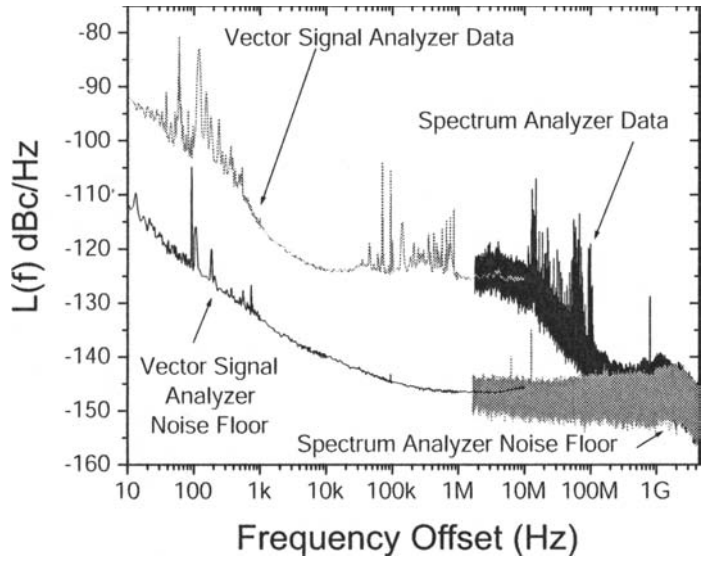

Fig. 12. Single-sideband phase noise of the hybridly mode-locked laser diode and corresponding noise floor. The plot is pieced together from vector signal analyzer measurements at low offsets and radio frequency spectrum analyzer measurements at high offsets. The measurement noise floor was obtained by bypassing the mode-locked laser and substituting it with an equivalent microwave loss (51 dB in this case) and was given by the thermal noise of the amplifiers after the photodiode. The mixer IF bandwidth was 2 GHz, which was wide enough to view the noise energy before it dipped below the measurement noise floor [4].

4.3. Characterization of Amplitude Noise

The intensity noise of an OTDM source can be measured by a fast photodiode and rf spectrum analyzer or by an AM noise measurement. The theory of RIN in cw semiconductor lasers is described in [68], but does not entirely apply to mode-locked lasers. The amplitude noise spectrum of mode-locked lasers also includes the correlated amplitude noise from the driving rf microwave oscillator.

4.3.1. Direct Detection and RF Spectrum Analyzer

The amplitude noise of cw laser diodes is often measured by detection with a fast photodiode followed by a low-noise rf amplifier and an rf spectrum analyzer. Using this technique, the RIN of a widely tunable sampled-grating DBR laser was measured to have less than -160 dB/Hz (at frequencies below the relaxation oscillation frequency) for optical powers above 1 mW [80].

The measurement of the amplitude noise of a mode-locked laser is more difficult since the rf power spectrum contains both amplitude and timing noise. Therefore, one must assume a model for the laser noise before interpreting the amplitude noise [70]. The uncorrelated amplitude noise for a fundamentally mode-locked laser appears as noise skirts around each harmonic with the same magnitude [71]. Since the measured

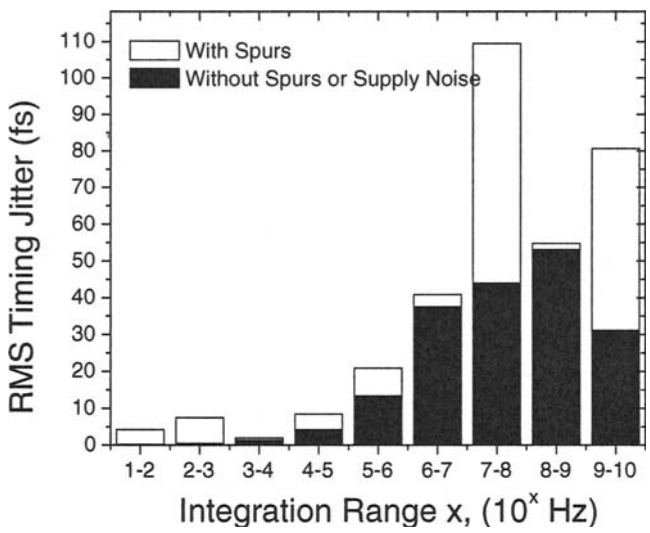

Fig. 13. The integrated timing jitter in each decade of the phase noise shown in Fig. 12. The square root of the sum of the squares of the numbers above yields the jitter over multiple decades. In the last decade, from 1 to 4.5 GHz, the white bar corresponds to the timing jitter where we assume that the noise is equal to the noise floor and the black bar corresponds to a theoretically expected -20 dB/decade rolloff [4].

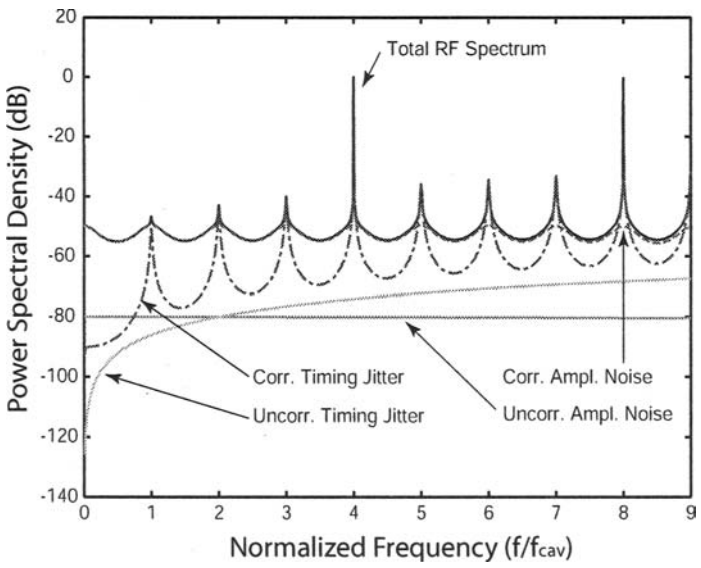

Fig. 14. RF spectrum of a harmonically mode-locked laser.

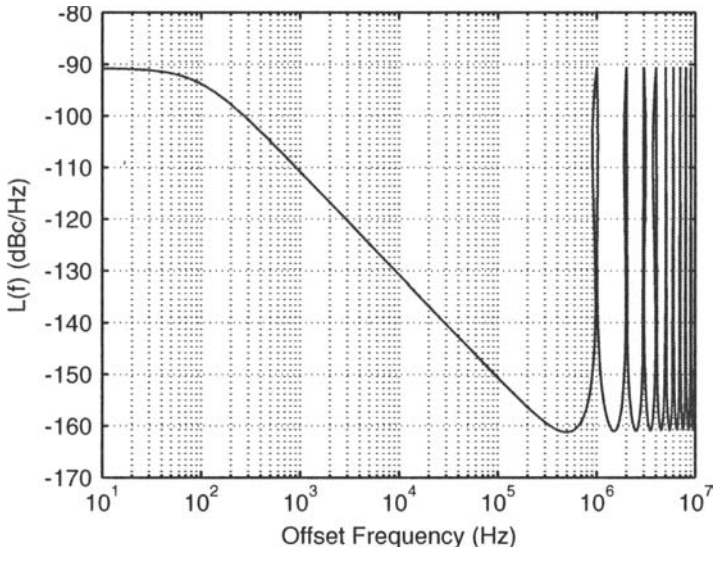

Fig. 15. Power spectral density of the timing jitter for an AM actively and harmonically mode-locked laser.

noise is a combination of both amplitude and timing fluctuations, it is difficult to extract the amplitude noise from this measurement alone.

4.3.2. AM Noise Measurement

The AM noise can be measured by downconverting the photodetected signal using the same rf oscillator used to drive the OTDM pulse source. The method relies on using a low noise mixer biased so that the LO and RF ports are in phase. The IF port yields a signal proportional to the amplitude noise.

The AM noise measurements of harmonically mode-locked [5] and fundamentally mode-locked [62] semiconductor lasers show that the amplitude noise of a mode-locked semiconductor medium has the usual broad band RIN noise spectrum with a peak at the relaxation oscillation frequency [68] plus correlated noise from the driving rf oscillator.

An overview of sensitive AM noise measurements of femtosecond Ti:sapphire lasers is presented in [81].

4.4. Low Noise Mode-locked Laser Design

4.4.1. Cavity Optimizations

The rms timing jitter of an actively mode-locked laser is [76]

$$\sigma_t^2 = \frac{\mathcal{E}_{\mathrm{ASE}}}{w_0} \frac{1}{2M\omega_M^2}, \tag{1}$$